

LaM CUBE

Laboratoire de mécanique,
multiphysique, multiéchelle



Journées Tribologie et Traitements de surface
22-23 novembre 2023, CETIM - SENLIS

Processus d'usure en freinage par friction : quelle clé pour atténuer à la source les émissions de particules ?

Yannick DESPLANQUES

Mathis BRIATTE, Asma GRIRA, Joseph FRANGHIE, Raafa AL-KADERI,
Edouard DAVIN, Alexandre MEGE-REVIL, Anne Lise CRISTOL, Jean François BRUNEL, Philippe DUFRENOY
Esperanza PERDRIX, Laurent ALLEMAN, Alexandre TOMAS
Florent BRUNEL, Laurent COUSTENOBLE, Arnaud BAURAIN



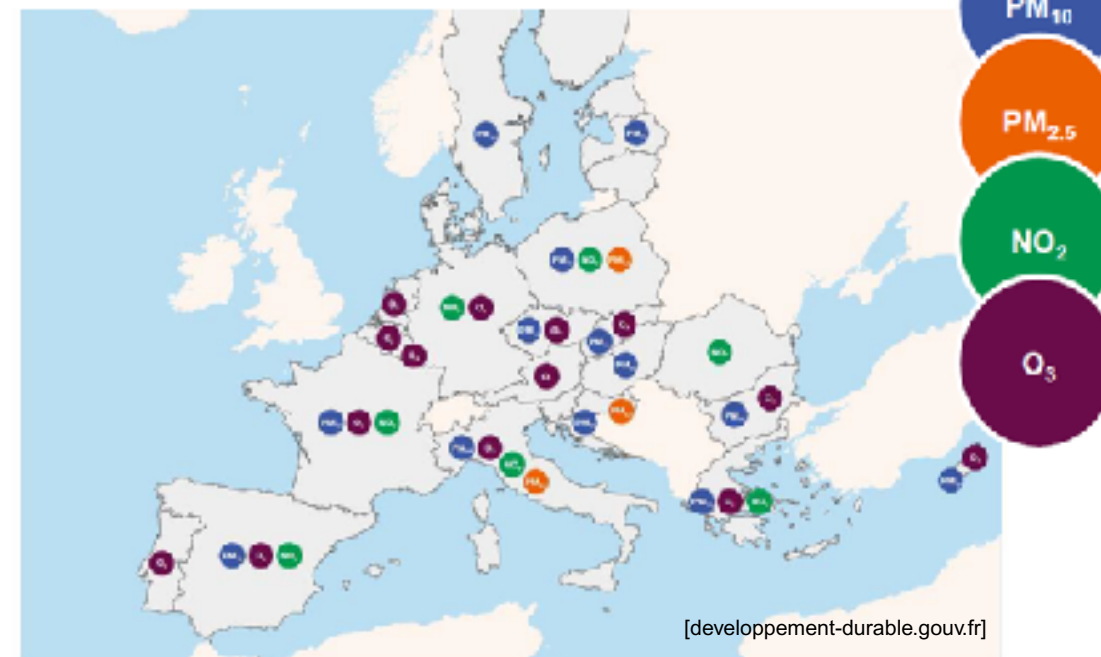
2

Context and issues

Air quality

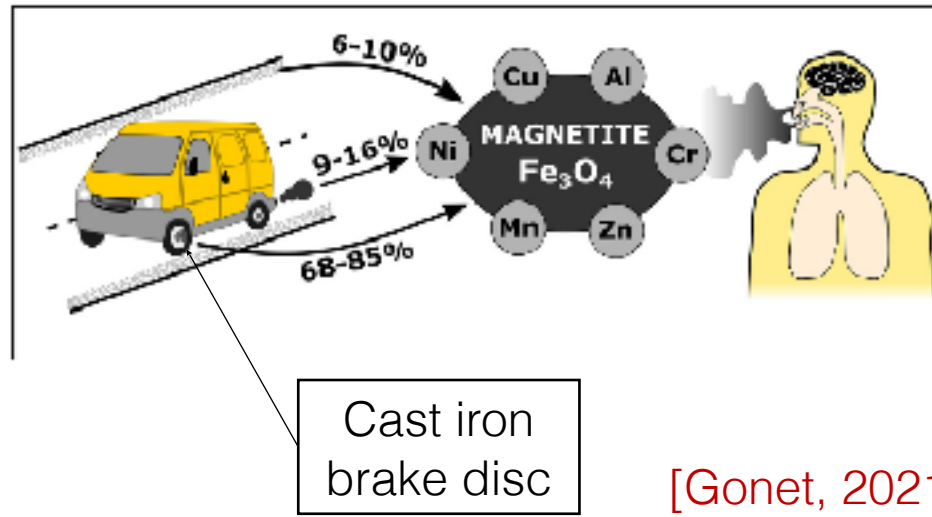
- Air Quality is a major concern in urban/suburban areas and in mobility
- Although improving for over 20 years, it still doesn't meet the WHO recommendations
- Poor Air Quality in urban centers leads to **238,000 premature deaths** (European Environment Agency).

Exceeding of the regulatory AQ thresholds in the EU in 2020

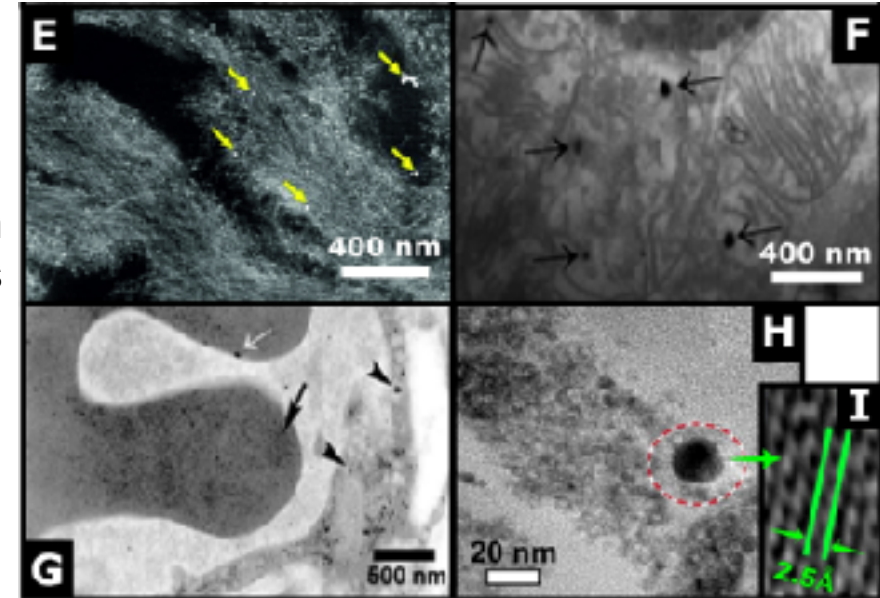




Context and issues Particle emissions - Automotive braking



Magnetite in neurons



Magnetite in the left ventricle of a human

Magnetite in the heart and red cells

[Gonet, 2021]

- Iron oxides could play a specific role in Alzheimer's disease [Maher, 2019]
- Limitation of particle emission from Euro7 Norm (European Commission) :
 - 7 mg/km until 2035.
 - 3 mg/km after 2035.



Context and issues Particle emissions - Railway braking

- Rail transport contributes to less than 1% of the total atmospheric particle emissions from all sources.
- However, in underground railway enclosures, these emissions lead to concerning particle concentrations.
- The main sources of these particles are largely attributed to railway activities (braking system, wheel-rail contact, ...)

PM: Comparison between outdoor (**Urban Air Ambient**)
and indoor (**Underground Rail Enclosures**)

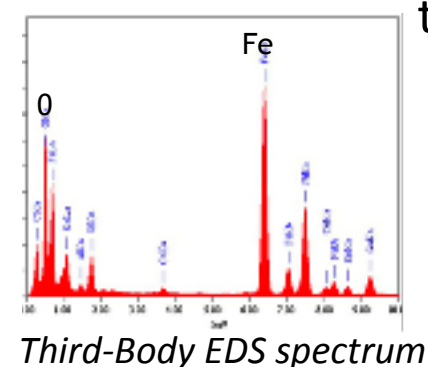
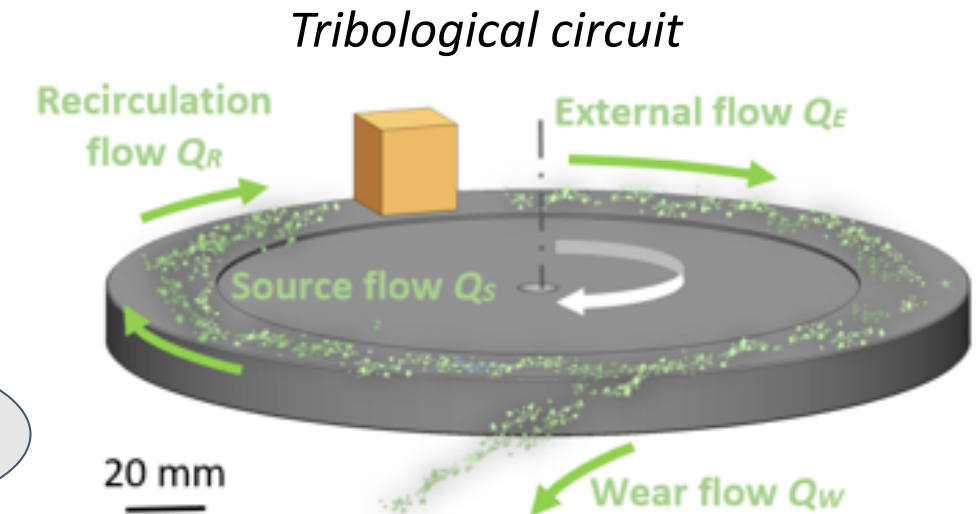
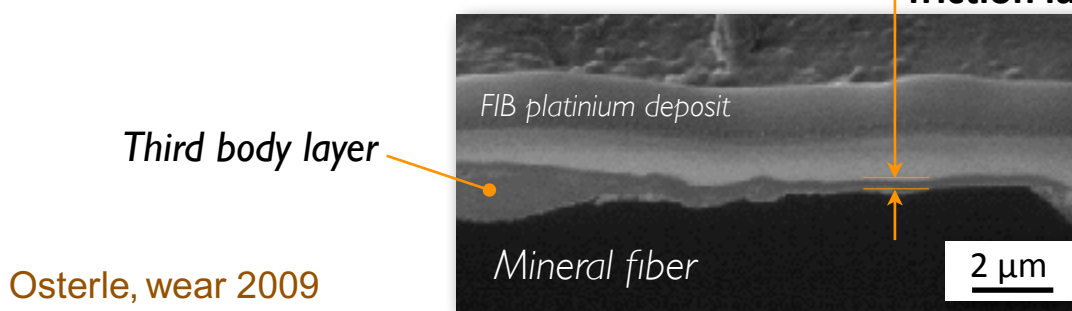
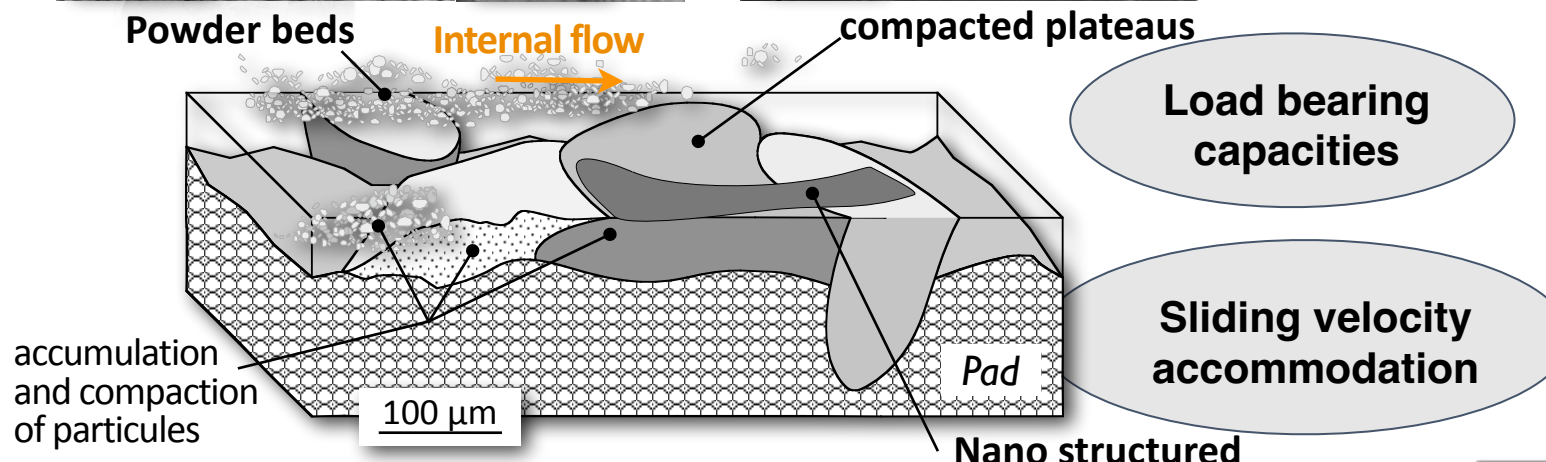
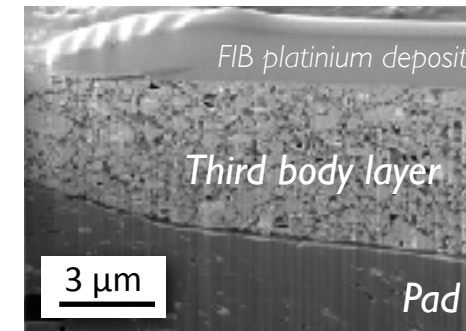
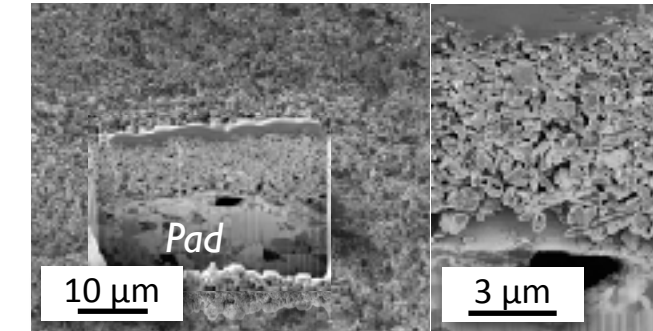
Ville	Année de mise en service	Année de mesure	Spèces mesurées	Niveaux intérieurs ($\mu\text{g.m}^{-3}$)	Niveaux extérieurs ($\mu\text{g.m}^{-3}$)	Référence
Barcelone	1924	2011	PM ₁₀ ; PM _{2,5}	346 ; 125	- ; 18	Querol et al. (2012)
	2009	2011	PM ₁₀ ; PM _{2,5}	145 ; 46	- ; 18	Querol et al. (2012)
Londres	1863	1996	SPM ; PM _{0,5}	669 ; 245	-	Pleifer et al. (1999)
		1999	PM _{2,5}	200	35	Adams et al. (2001)
Los Angeles	2000	2010	PM ₁₀ ; PM _{2,5}	78 ; 57	31 ; 20	Karn et al. (2011a)
Paris	1880	2016	PM ₁₀ ; PM _{2,5}	207 ; 79	20 ; 12	AFF (2017)
	1999	2016	PM ₁₀ ; PM _{2,5}	38 ; 13	20 ; 12	AFF (2018)
Prague	1974	2002	PM ₁₀	103	85	Braník (2006)
		2013	PM ₁₀ ; PM _{2,5}	205 ; 94	-	Cusack (2015)
New York	1904	1999	PM _{2,5}	52	13	Chillrud et al. (2004)
		2004	PM _{2,5}	52	-	Grass et al. (2010)
Stockholm	1964	2004	PM _{2,5}	52	-	Grass et al. (2010)
Seoul	1974	2005	PM ₁₀ ; PM _{2,5}	350 ; 129	155 ; 102	Kim et al. (2008)
	1985	2014	PM ₁₀ ; PM _{2,5}	214 ; 78	44 ; 14	Lee et al. (2018)
Shanghai	1993	2008	PM ₁₀ ; PM _{2,5}	366 ; 193	-	Ye et al. (2009)
	2010	2012	PM _{2,5}	64	66	Lu et al. (2015)
Taipei	1997	2010	PM ₁₀ ; PM _{2,5}	58 ; 33	44 ; 30	Cheng et Yan (2011)
Tokyo	1927	1997	SPM	120	-	Furuya et al. (2001)

[Durand,2021]

Context and issues

Tribological circuit and mechanisms involved by braking

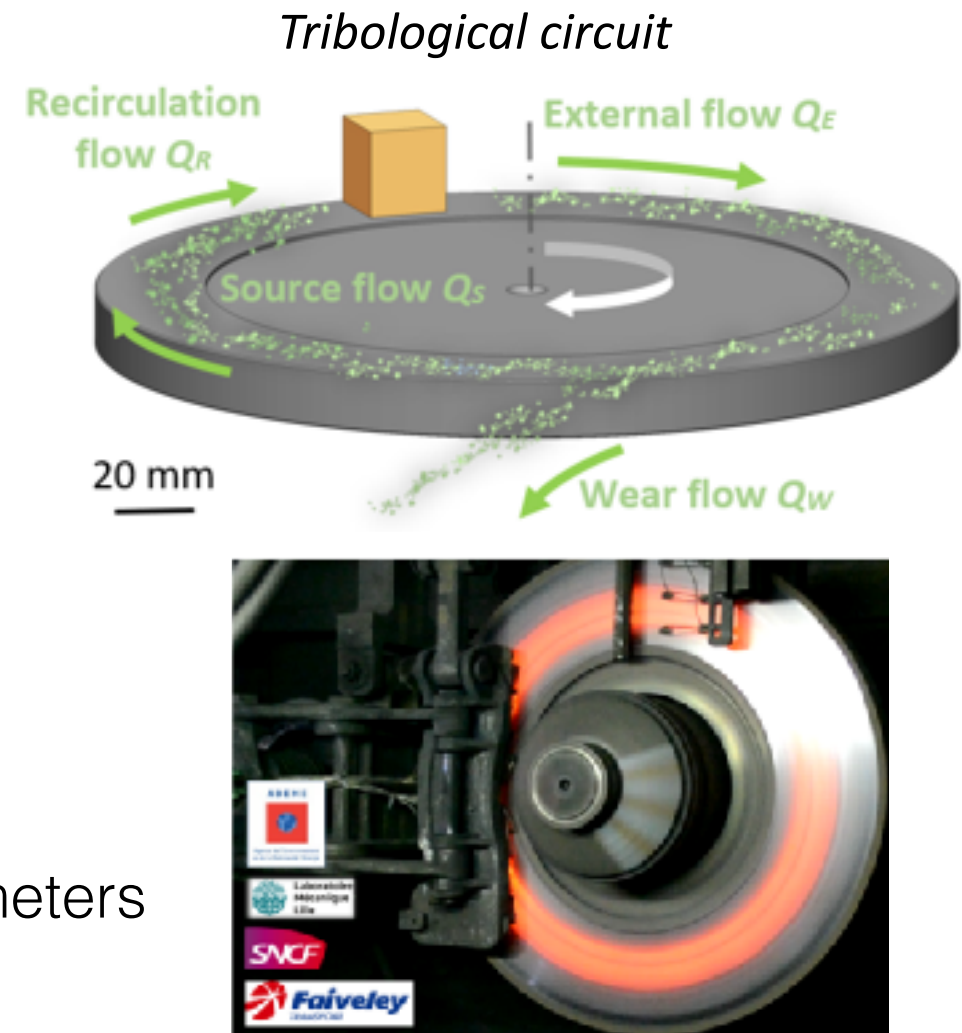
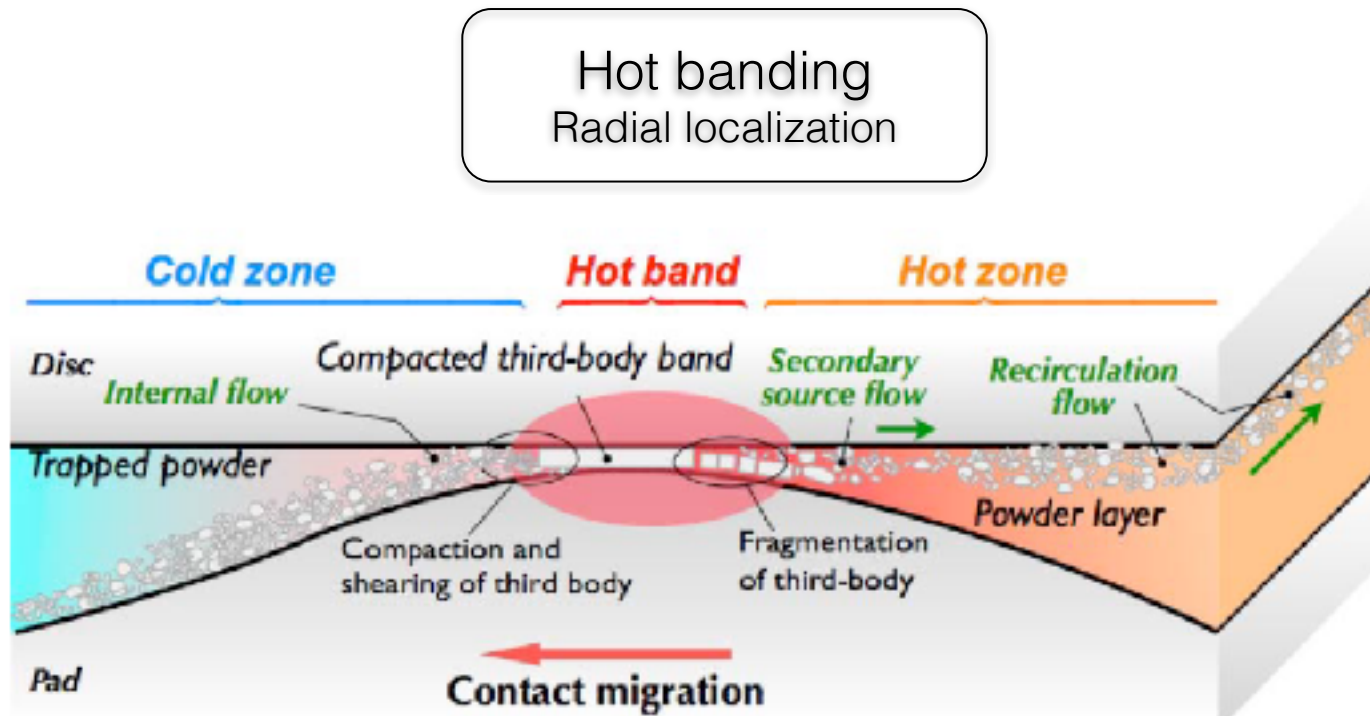
5



Main source of particles:
tribo-oxidation of the disc



Context and issues Tribological circuit and mechanisms involved by braking



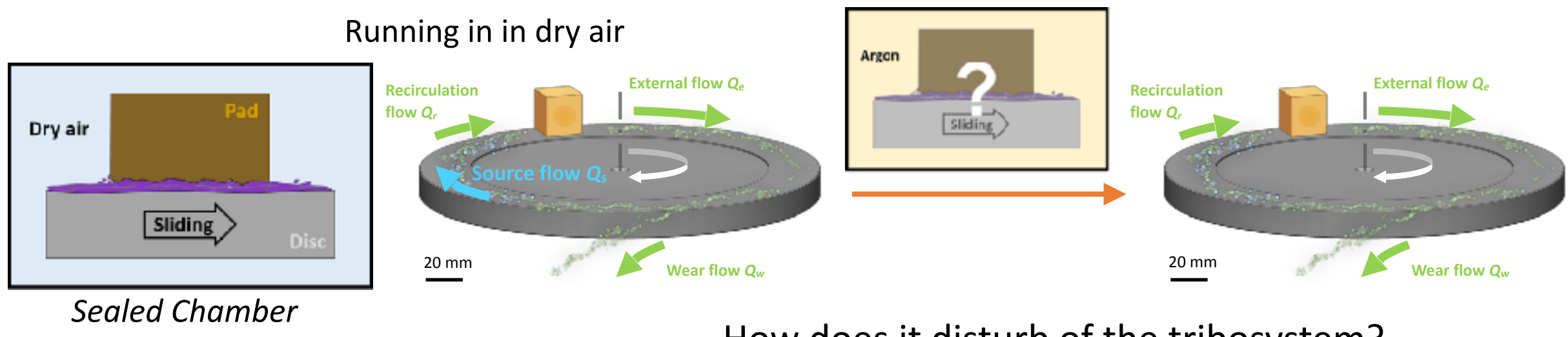
Effect of the tribosystem parameters

- What is the relation between the third body flows and the particle emission?



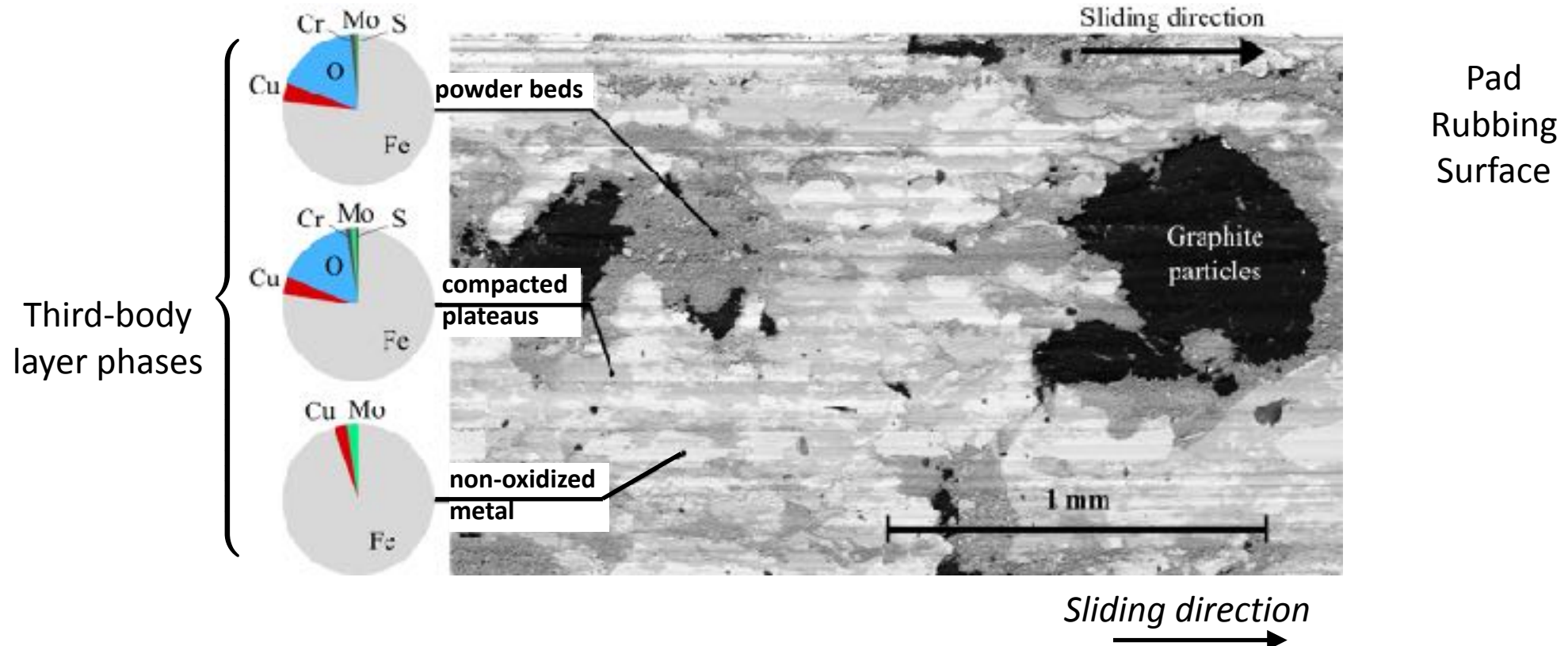
Example 1 Evidence of third-body source flow

- Friction material paire: sintered FeCu-matrix composite pad - 15CrMoV6 steel disc
- Sequences of 20 friction tests (8 m/s, 200 N, contact area 20 x 20 mm)
- First stage: running in in dry air
 - development of a third-body layer representative of braking situations
- Second stage: running-in in argon
 - change of the tribological matter balance by removing the oxidative source flow





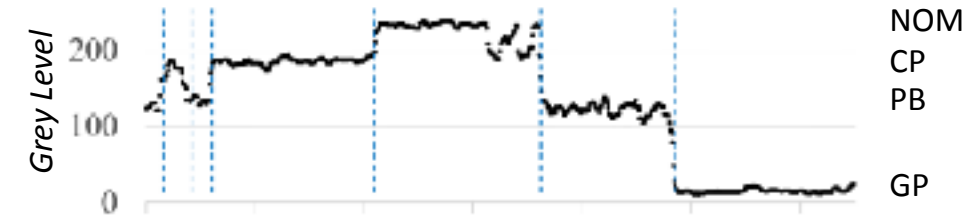
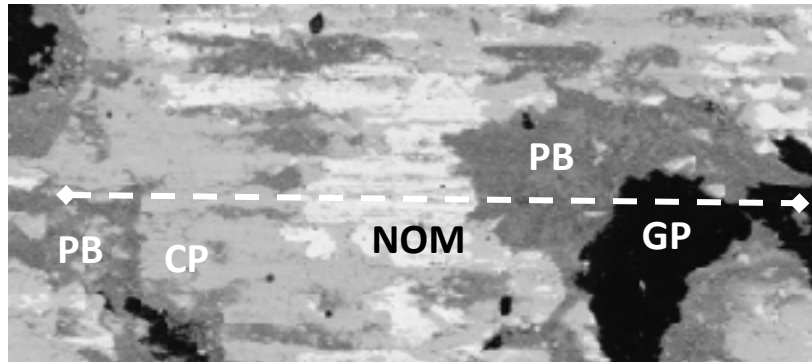
Third-body layer after running-in in dry air



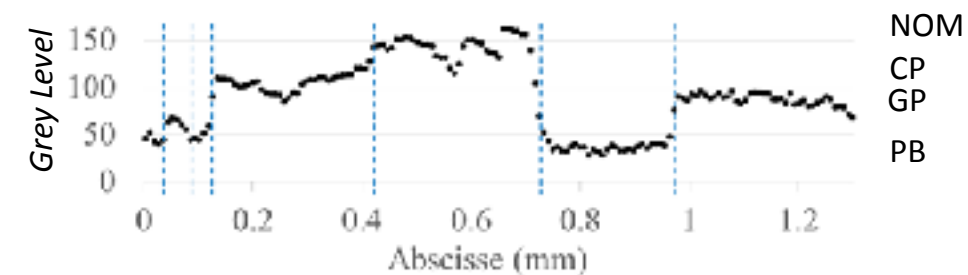
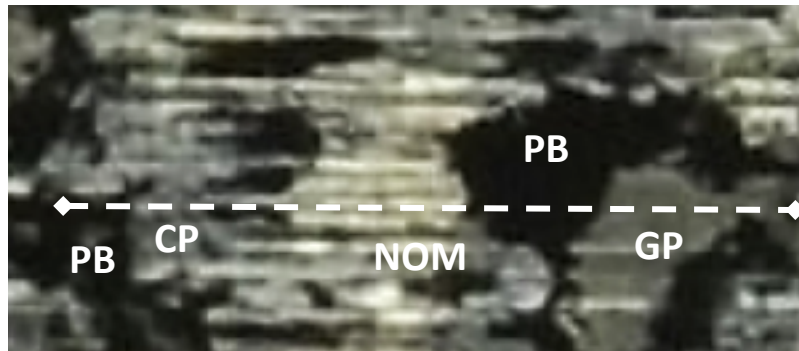
- Powder beds and compacted plateaus: mainly iron oxides mixed with pad and disc elements
- non-oxidized metal: mixture of iron with elements from pad (Cu) and disc (Mo)



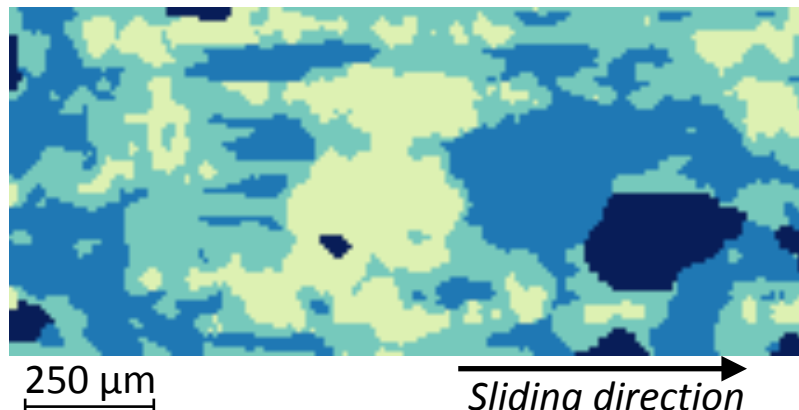
Mapping of surface composition using image analysis



SEM BSE image



Photograph

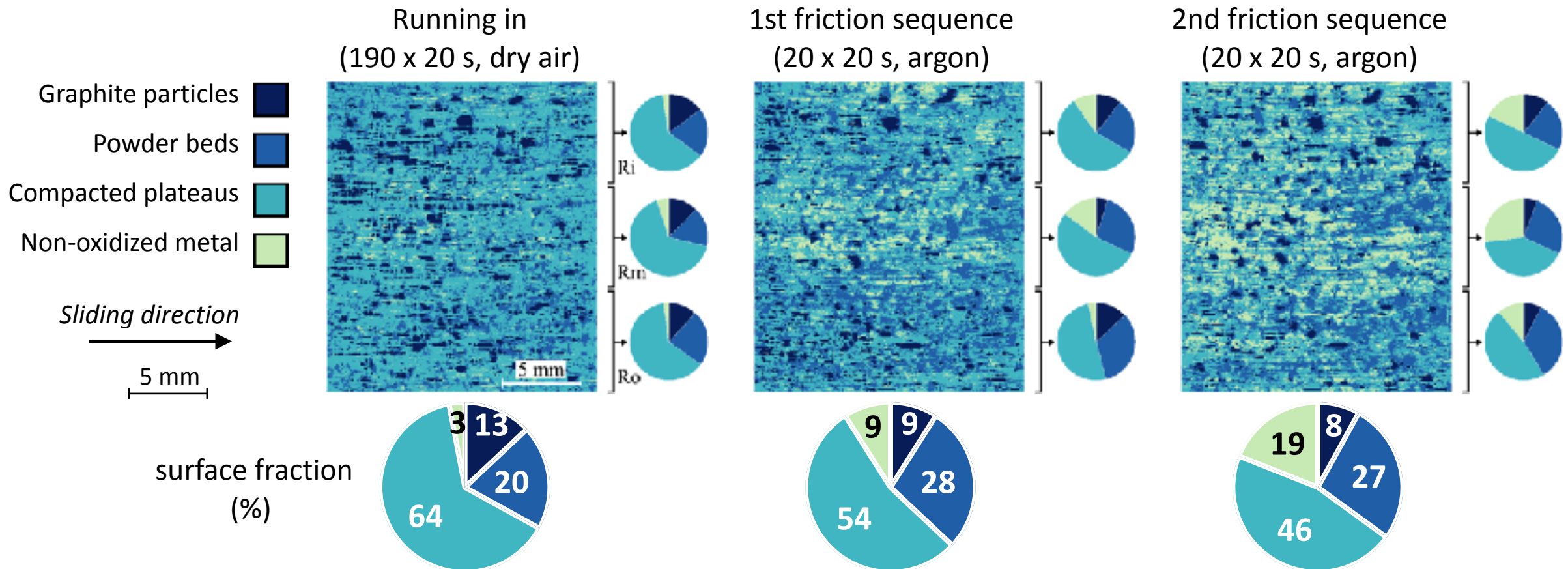


- graphite particles (GP)
- powder beds (PB)
- compacted plateaus (CP)
- non-oxidized metal (NOM)

Colored map



Evolution of pad friction surface

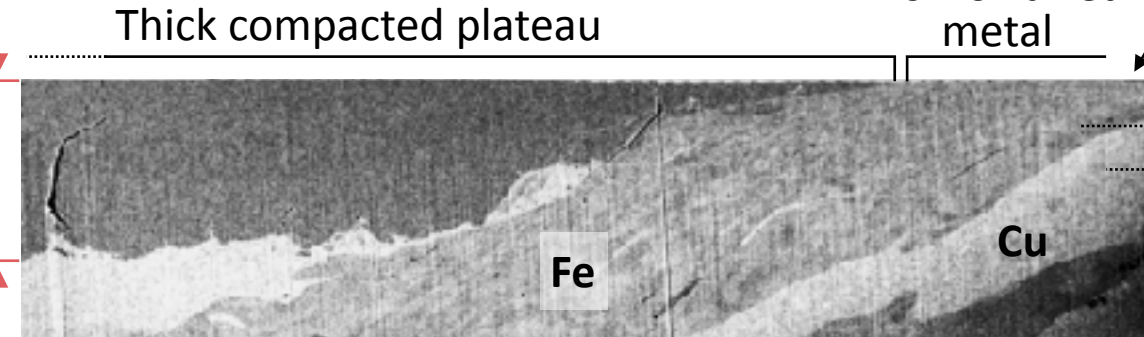


- When oxidative source flow of third body is reduced:
 - areas of compacted plateaus decrease
 - areas of non-oxidized metal increase
 - areas of powder beds and graphite remain rather constant

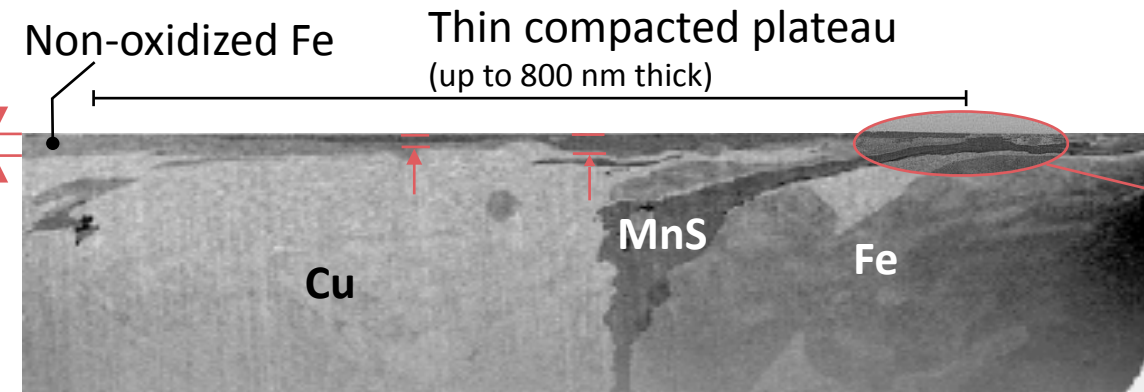


Third body layer in dry air

Fib cut ①

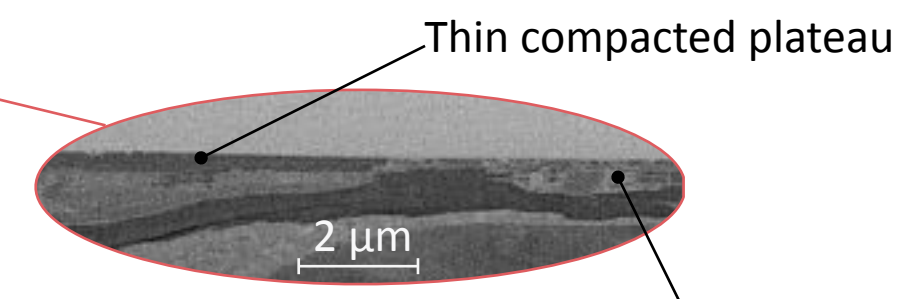
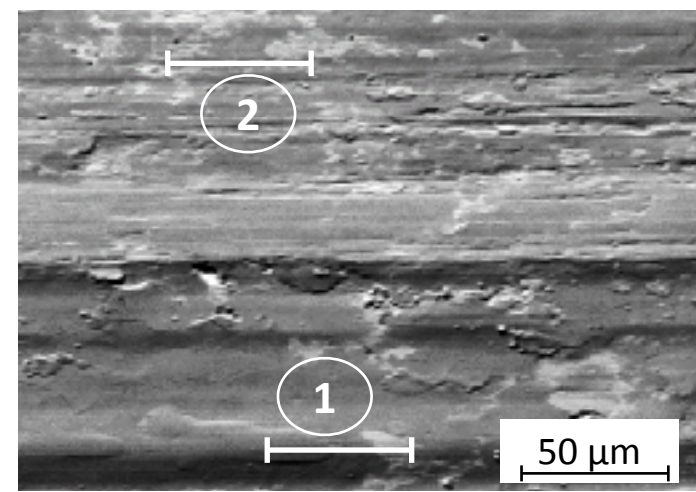


Fib cut ②



10 µm

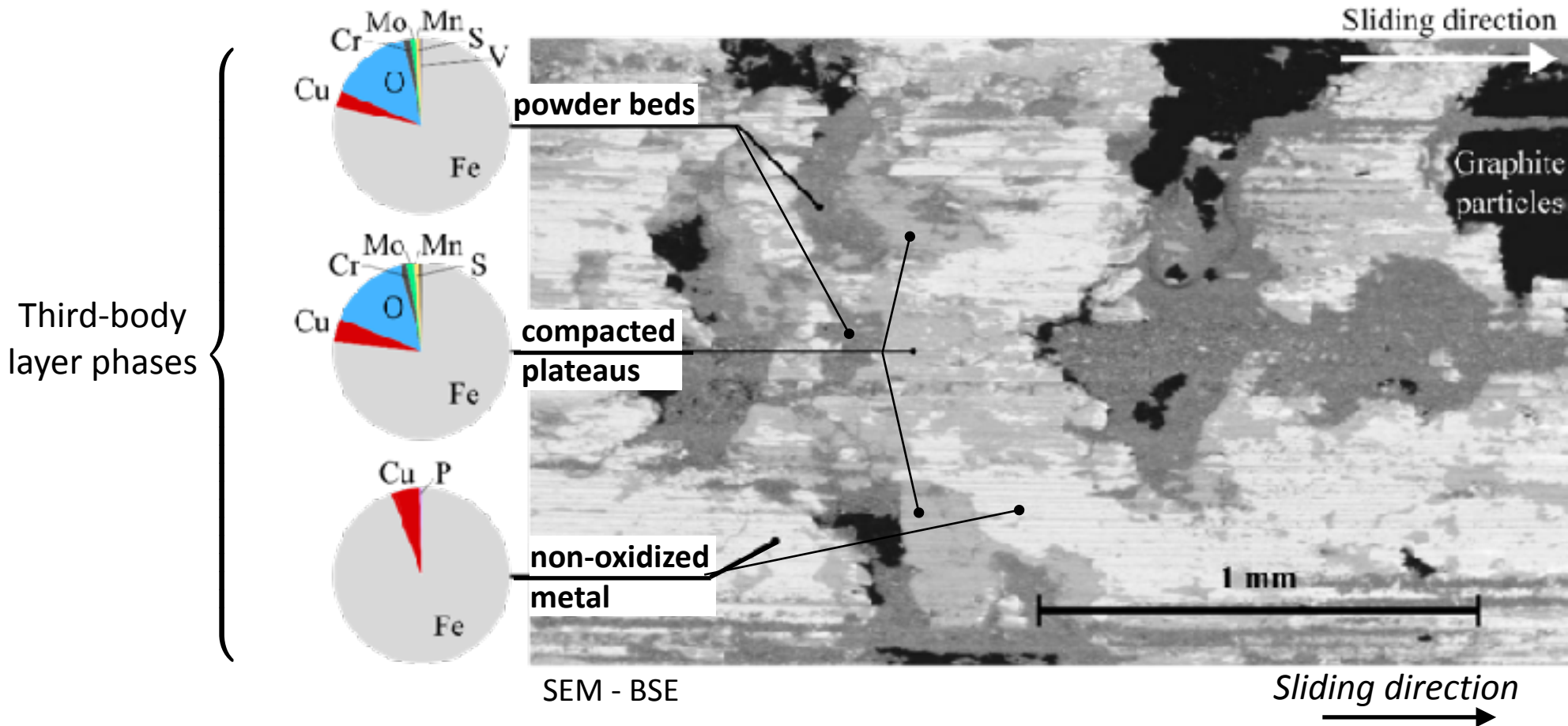
FIB cut location



- Compacted oxidized third body consists of:
 - thick plateaus formed in surface porosities where power beds are trapped
 - thin plateaus covering large areas of the friction surface
- Non-oxidized metal layers result of high plastic deformation and mixture of pad-disc particles



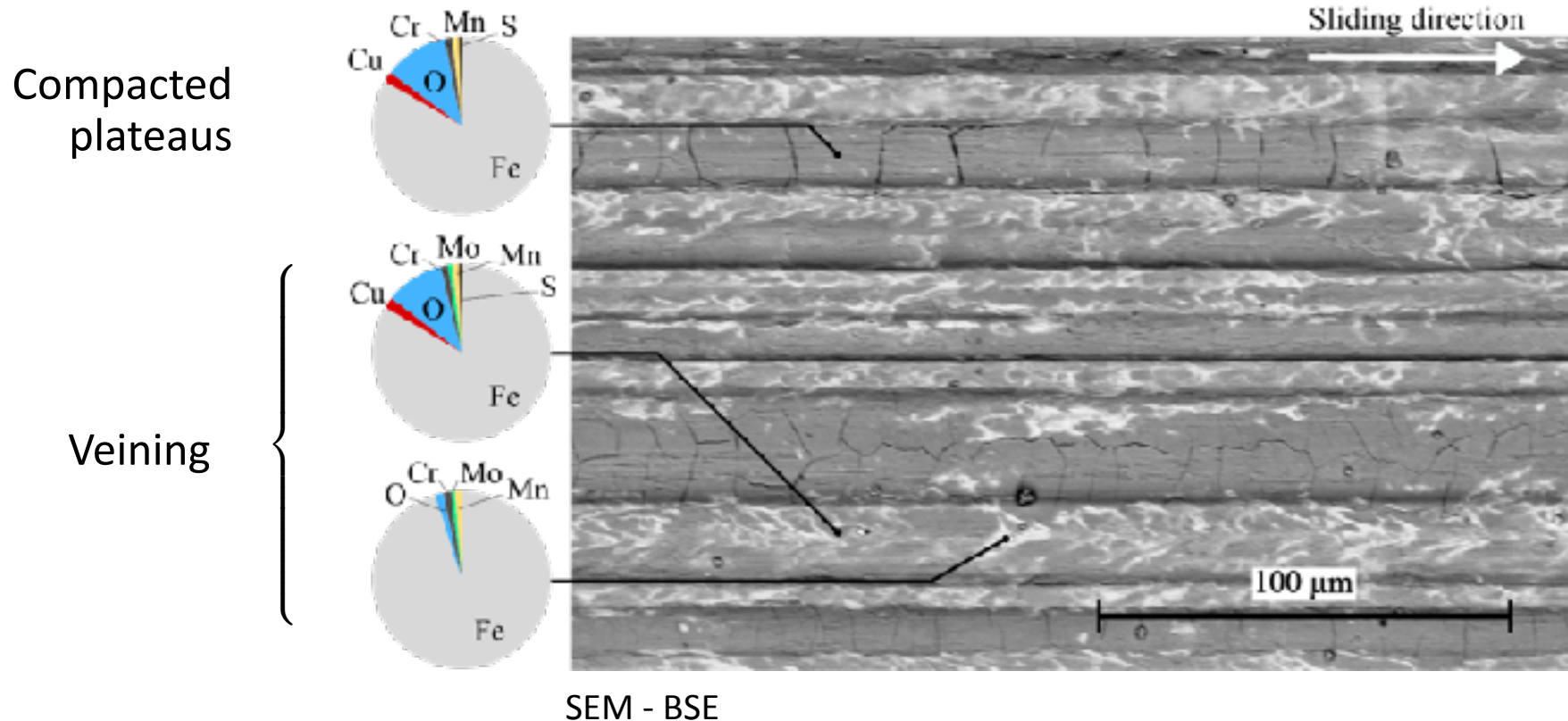
Third body layer change in argon



- less extent of the compacted plateau layer downstream powder beds
- development of the non-oxidized metal phase downstream compacted plateaus



Third body layer change in argon - disc surface



- Thick compacted plateaus remains trapped inside disc grooves
- Veining corresponds to alternance of thin compacted plateaus and non-oxidized metal
- Lack of powder beds

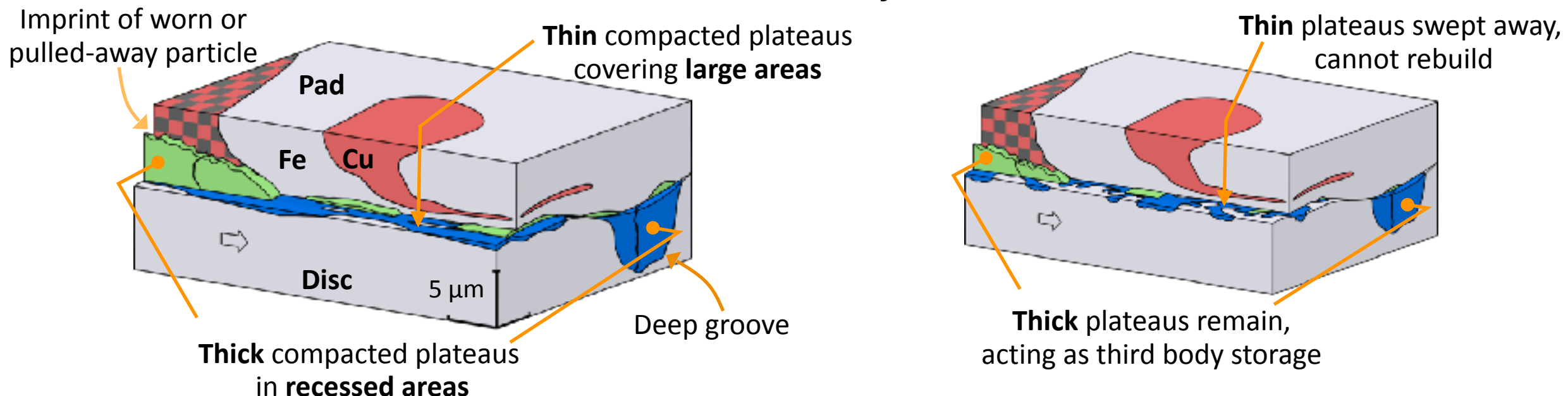


To conclude

Schematization of wear mechanisms alteration

Third-body layer in braking situation *Oxidative source flow reduction* → Altered load-bearing capacities

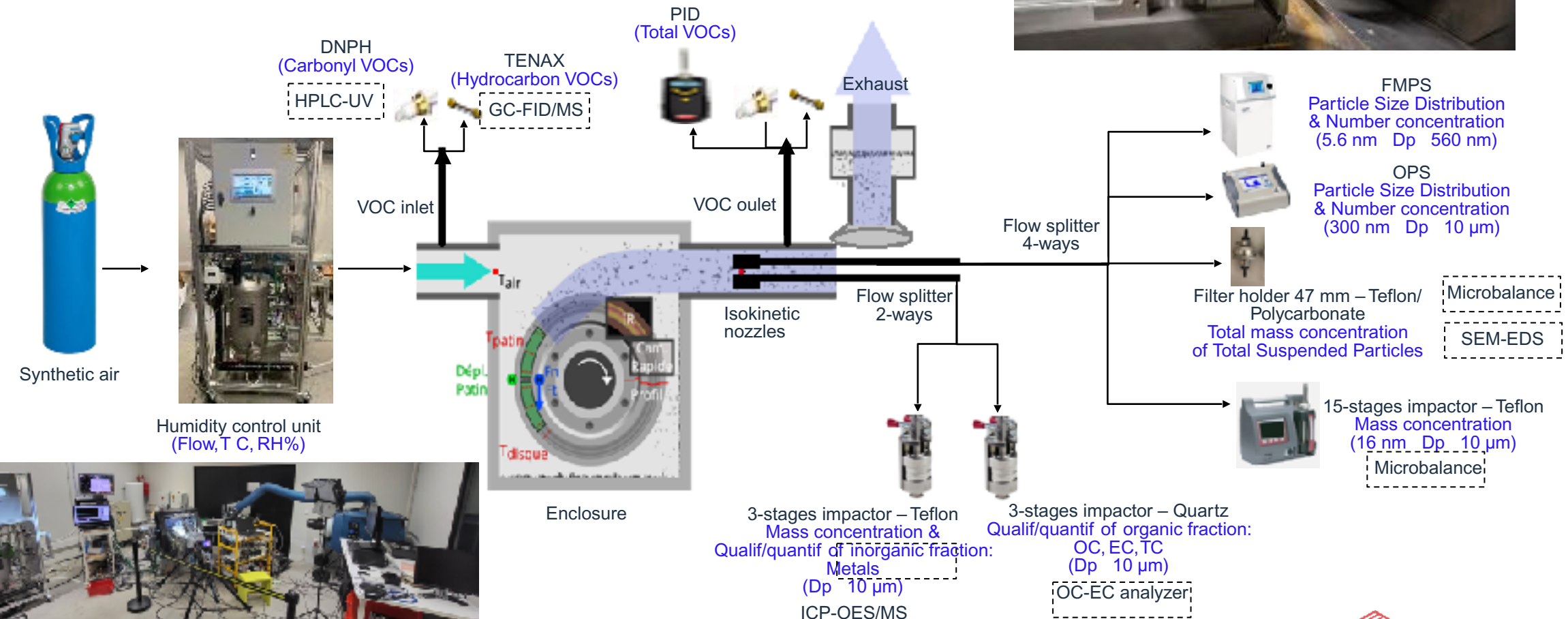
Imbalance between source and wear flows



The evolution of third-body flows changes load-bearing capacities in nature and extent, becoming more heterogeneous with a decrease of compacted third-body plateaus.



Braking emissions Experimental set up



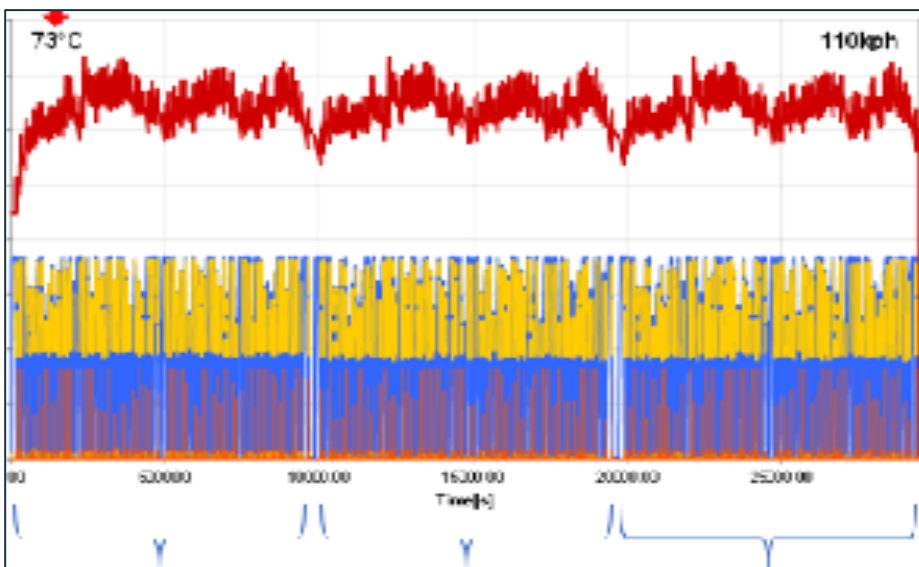


Exemple 2

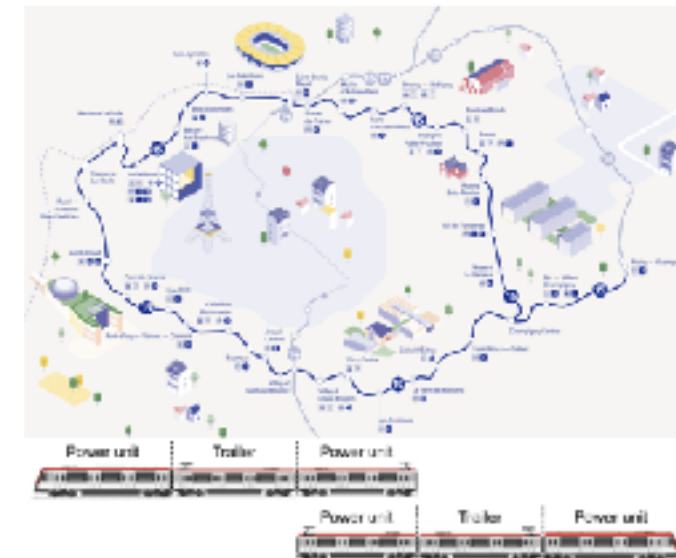
Simulation d'une journée d'exploitation d'une ligne de métro

16

Grand Paris Express - Ligne 15



3 allers-retours - 216 arrêts
9h d'exploitation - 450 km



*Thèses en cours Joseph FRANGHIE
Raafa AL-KADERI
Post-Doc Asma GRIRA*

**BREAQ – BRaking Emissions characterization
& mitigation for Air Quality improvement**

ALSTOM

RÉPUBLIQUE
FRANÇAISE
L'Etat, l'Assemblée
Nationale

FRANCE 2030

ADeme
Bureau des recherches

Study and characterization
of brake wear and emissions



Mitigation

ALSTOM FLERTEX

LaM CUBE
Laboratoire de mécanique
multiphasique, multiéchelle

IMT Nord Europe
Ecole Mines-Télécom
IMT-Université de Lille

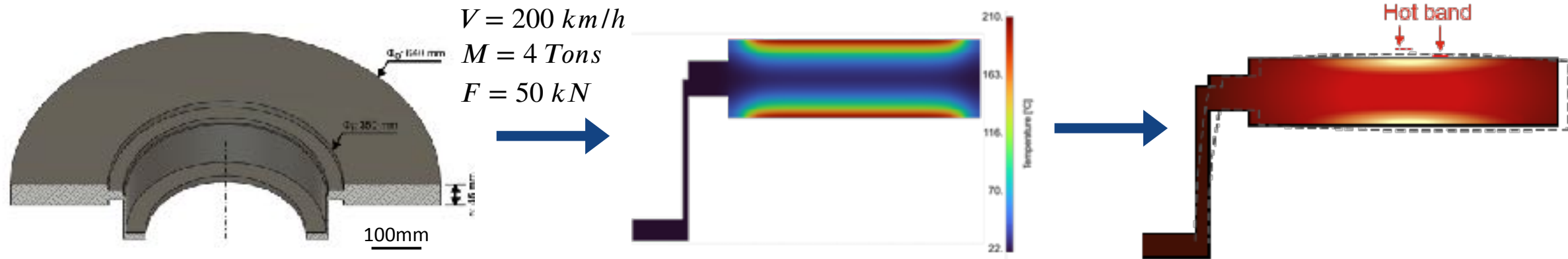
LNNIH

LaM CUBE
Laboratoire de mécanique,
multiphasique, multiéchelle

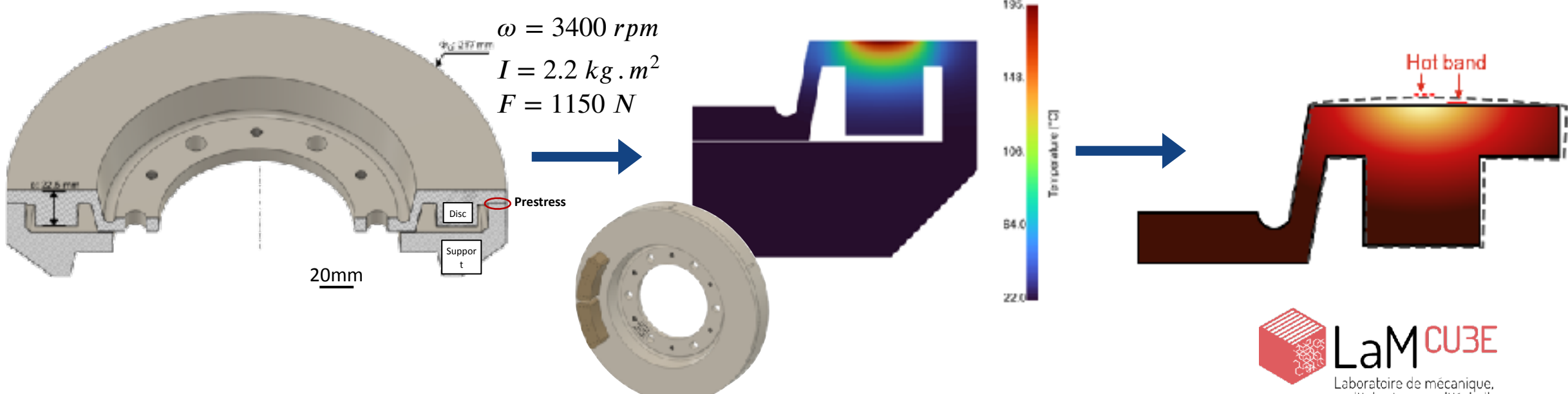


Réduction d'échelle - approche thermomécanique Reproduction de la sollicitation en bande chaude

- Full scale braking



- Pad on disc designed for reduced scale:

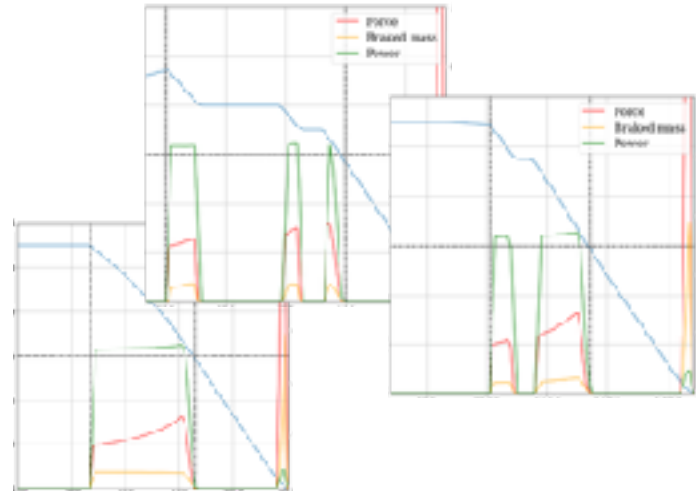




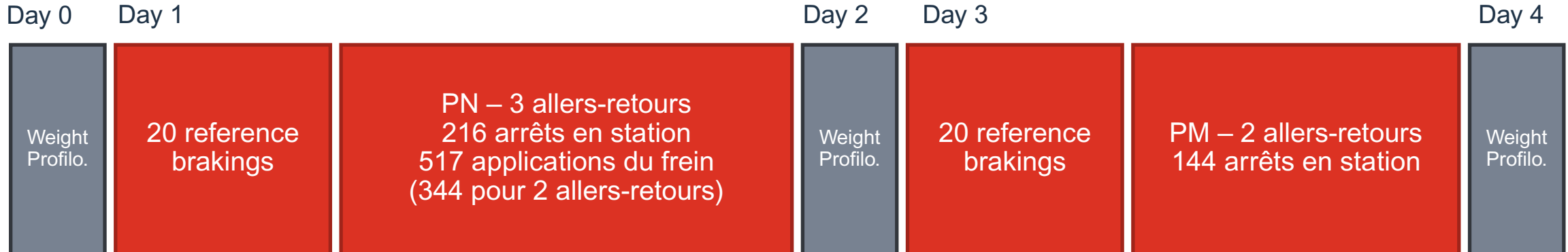
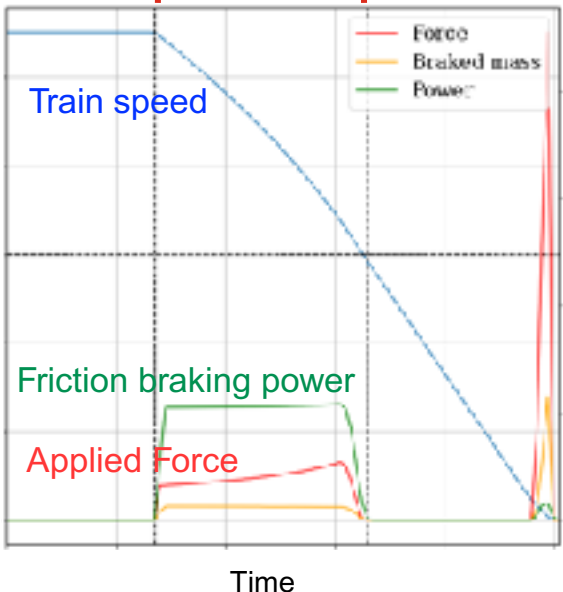
Procédure d'essai

- Parcours en exploitation Normale PN
 - 3 allers retours
 - 216 arrêts - diversité de freinages
- Parcours Modèle PM
 - 2 allers retours (144 station stops)
 - Reference braking
 - Real inter-braking time extracted from PN
- Reference braking series:
 - 20 x Braking of PM
 - Fixed inter-braking time (set to 60s)

Freinages de service - PN
Diversité des arrêts
Conjugaison frein électrique



Freinage de référence - PM
une seule application du frein



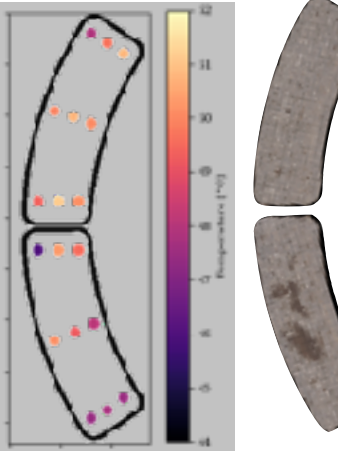
Evolution de la portance - frottement - usure du patin

« Premiers résultats »

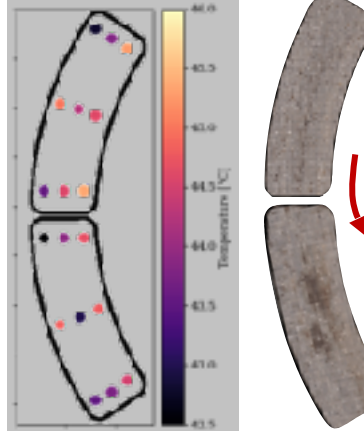
Après rodage
portance localisée
en sortie de
contact



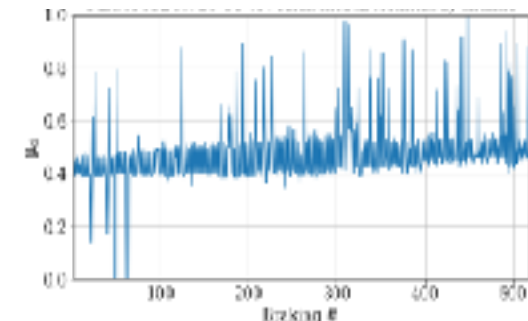
Pendant PN : relocalisation progressive de la portance sur le demi patin d'entrée de contact



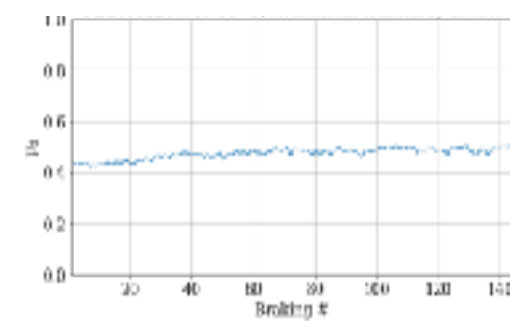
Pendant PM : portance installée, localisée sur le demi patin d'entrée de contact



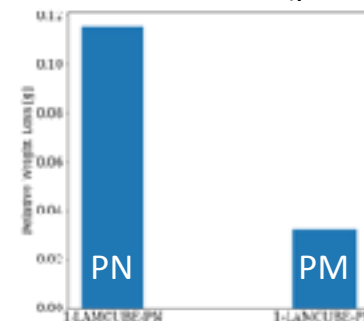
Frottement PN



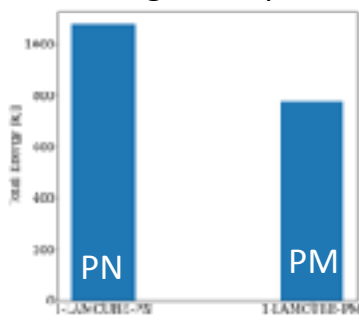
Frottement PM



Perte de masse (patin)



Energie dissipée



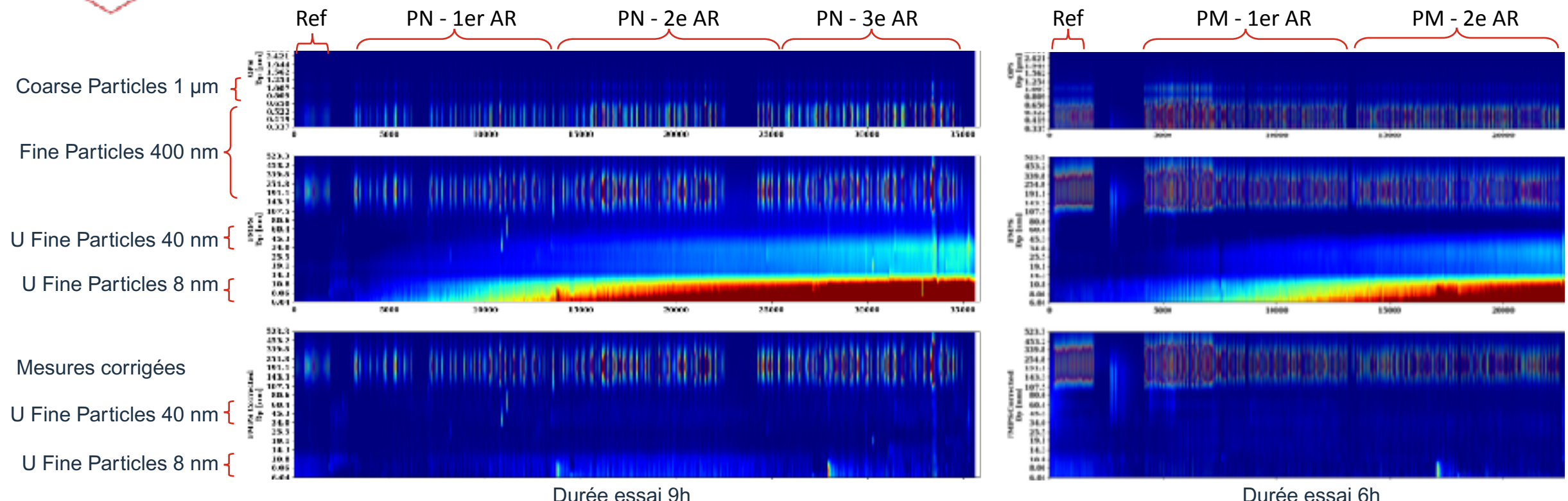
	PN	PM
Total energy [MJ]	1,078	0,78
# braking applications	517 (344 / 2 AR)	144
Pad weight loss [g]	0,115	0,032
Rate [g/MJ]	0,107	0,041
Sliding distance [m]	In Progress	

Quels sont les facteurs de perte de masse ?

- circuit tribologique:
 - adaptation de la portance
- usage du frein:
 - diversité des freinages
 - multiplicité des applications du frein
- design du frein:
 - 2 demi patin



Evolution des émissions



Quelle relation usure - émissions ?

- circuit tribologique:
 - historique de freinage, cumul troisième corps
 - capacité de stockage du troisième corps
- usage du frein:
 - diversité et multiplicité des applications du frein
 - multiplicité des applications du frein
- design du frein:
 - ouverture - fermeture du contact



Example 3

Simulation of repetitive low-energy urban slowdowns (from 50 to 20 kph)

21

- Experimental set up and testing protocol

Materials

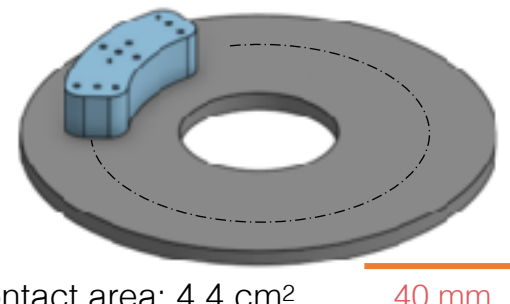
a single organic pad
2 disc materials:

Cast iron
Stainless steel

Braking conditions

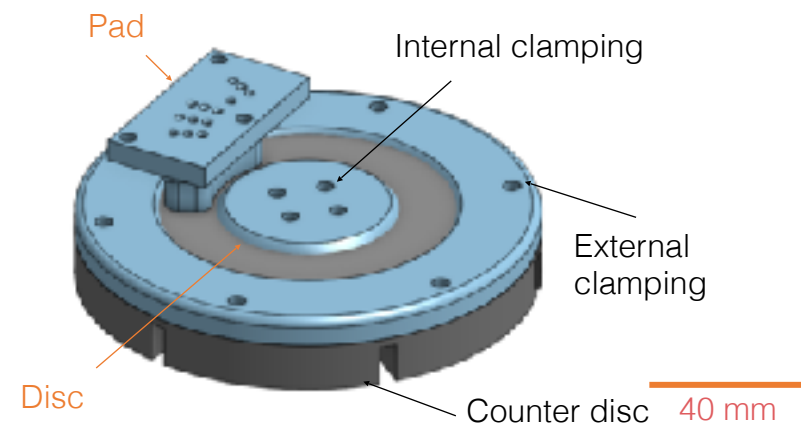
Series of 50 slowdowns
of 12 s and 13.7 kJ per
slowdown

Contact geometry

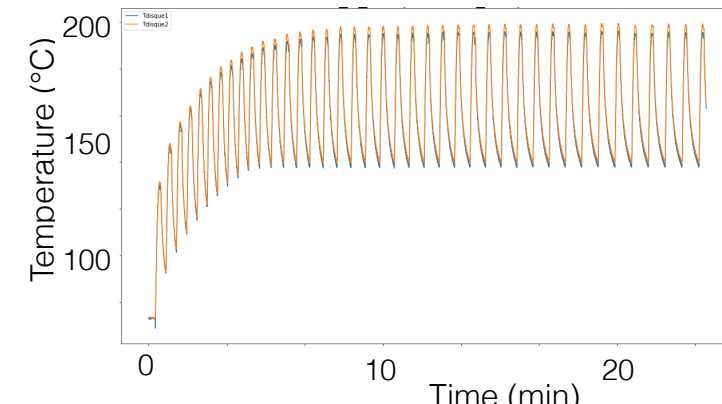
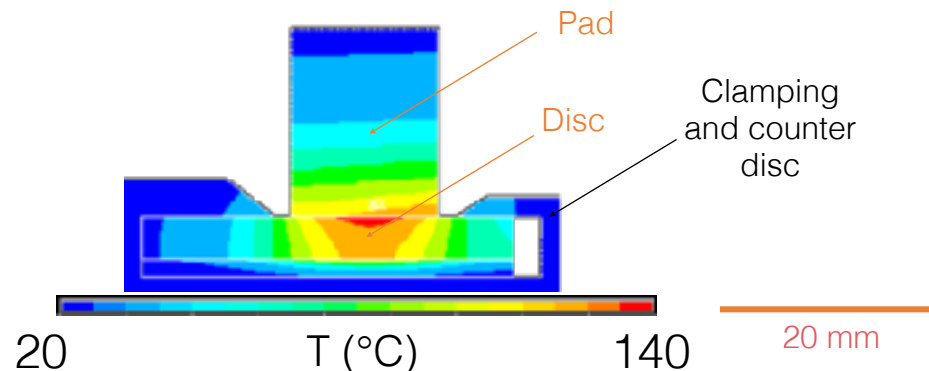


Contact area: 4.4 cm²
Disc thickness: 4.5 mm

Pad - Disc assembly



- Contact loading like real-life automotive braking - hot banding situation



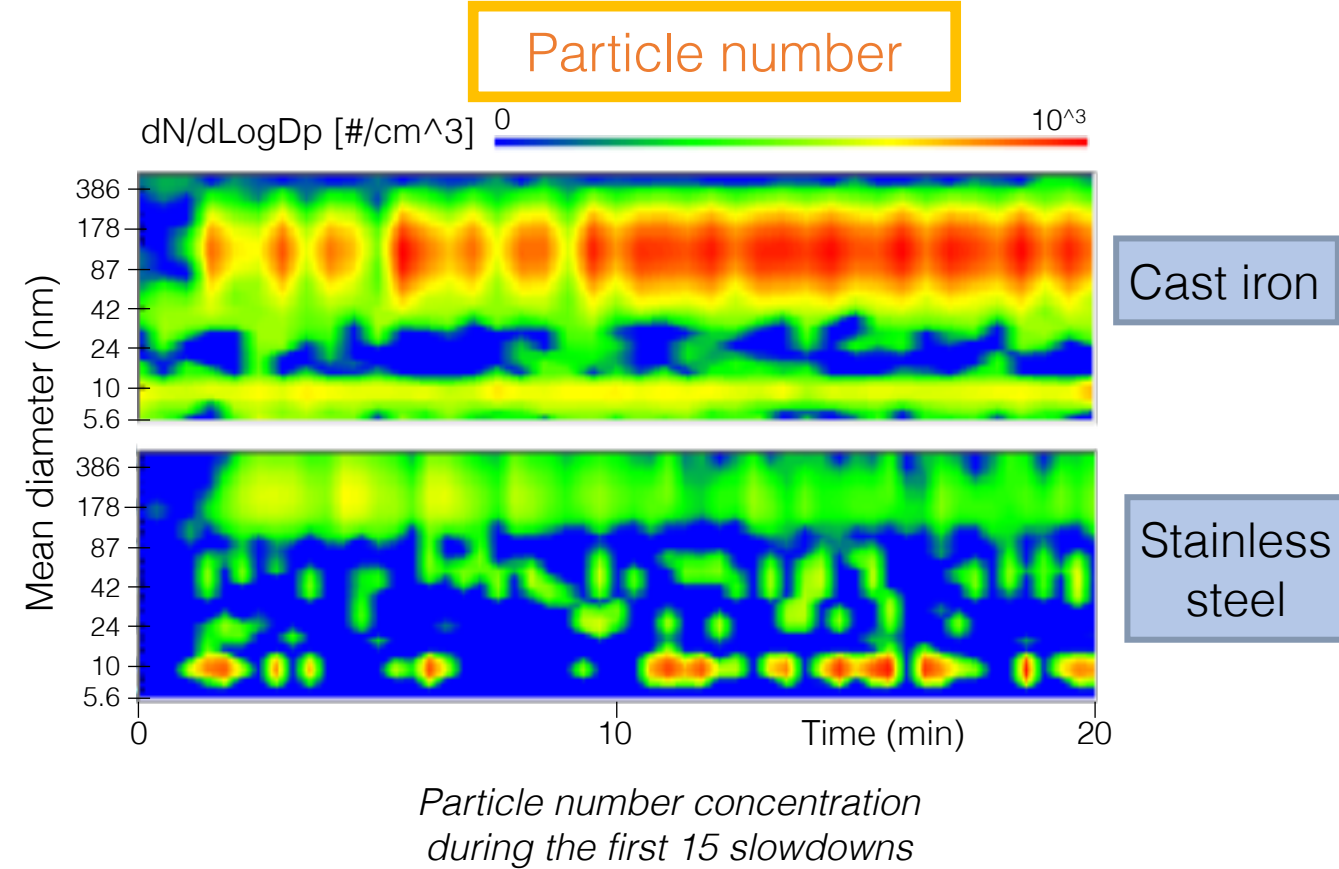
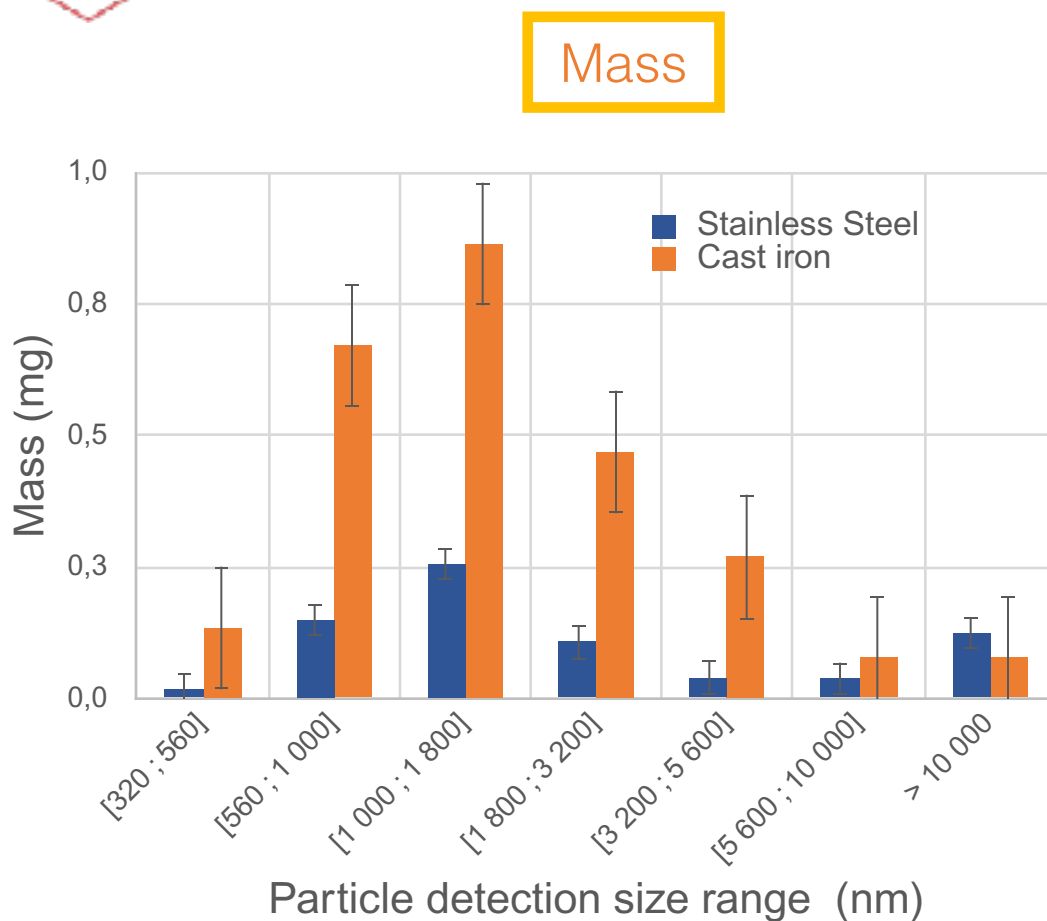
Thèse Mathis BRIATTE en cours

aperam

 **LaM CU3E**
Laboratoire de mécanique,
multiphasique, multiéchelle



Particulate emission - comparative study

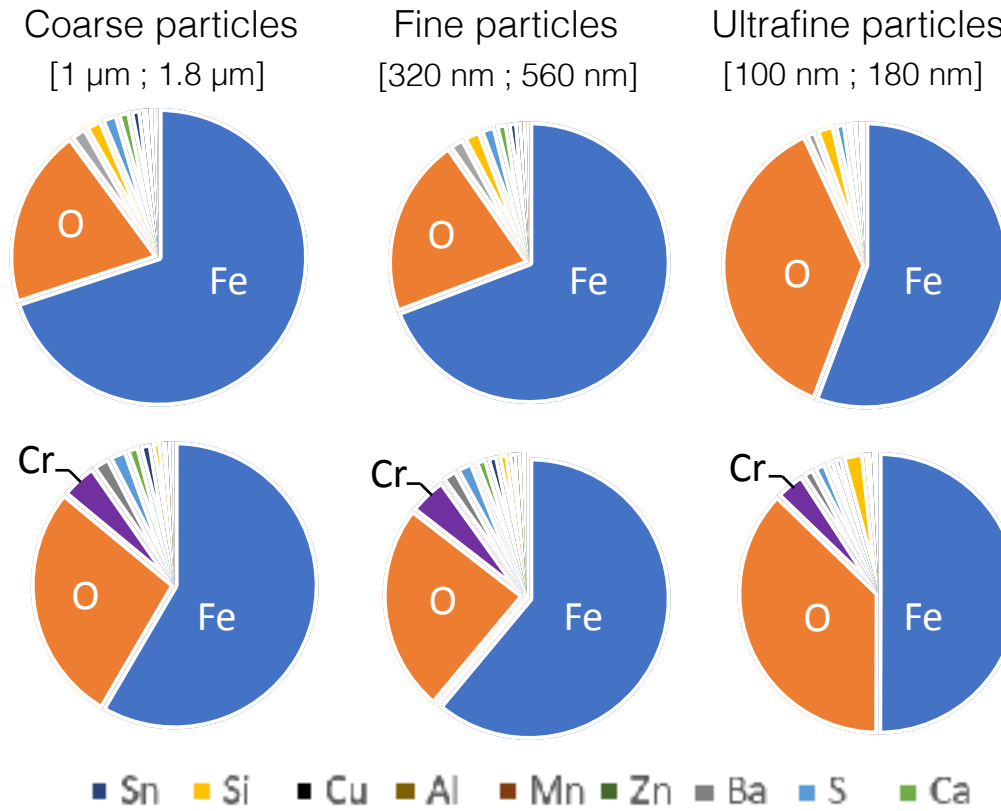


- Particulate emission involves mainly fine and coarse particles.
- Particulate emission is higher for cast-iron discs than for stainless steel discs.

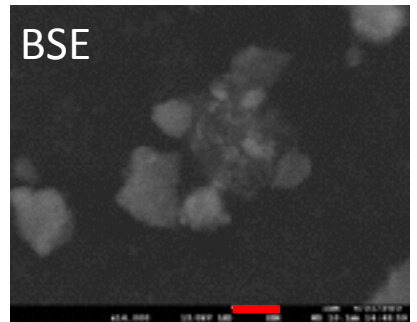


Particulate emission - comparative study

Cast iron

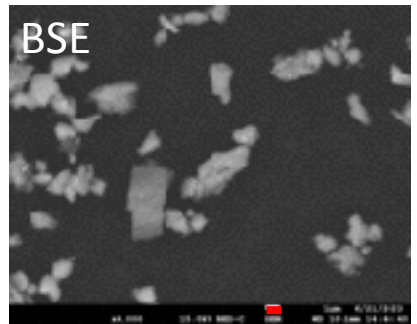


Stainless steel

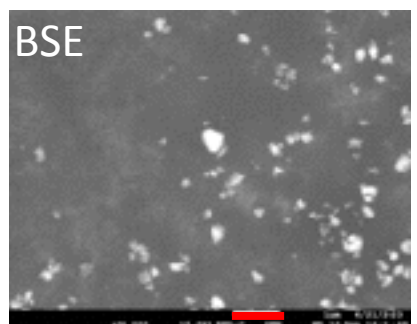


Morphology

Coarse particles and agglomerate



Fine particles elongated & angular shape



Ultrafine particles spherical shape

1 µm

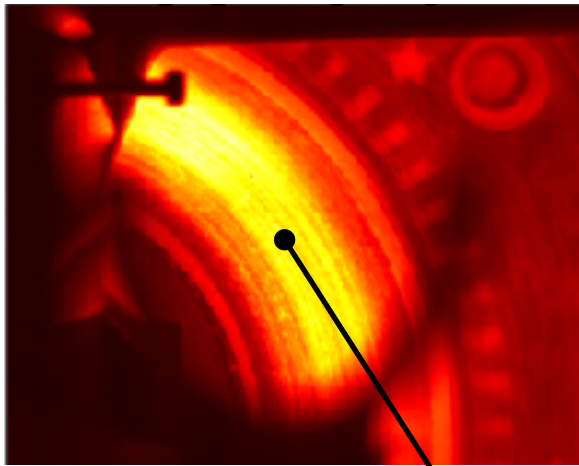
How to explain the difference in particle emissions?



Friction & thermomechanical loading

Cast iron

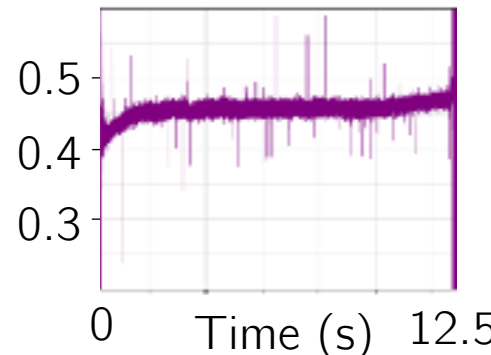
Disc-track IR thermogram



20 mm

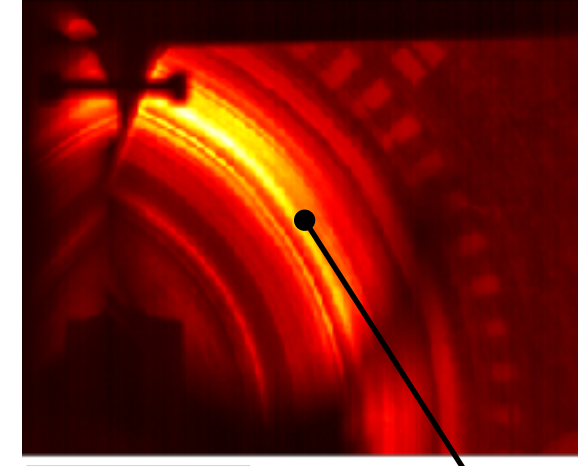
Hot band

Coefficient of friction



Stainless steel

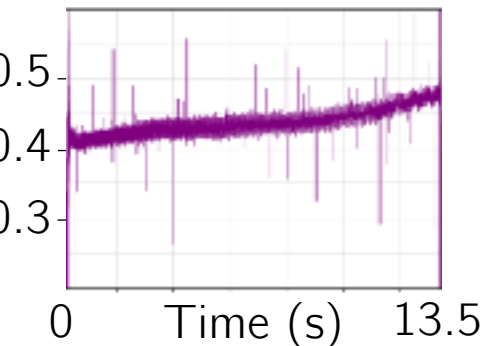
Disc-track IR thermogram



20 mm

Hot band

Coefficient of friction

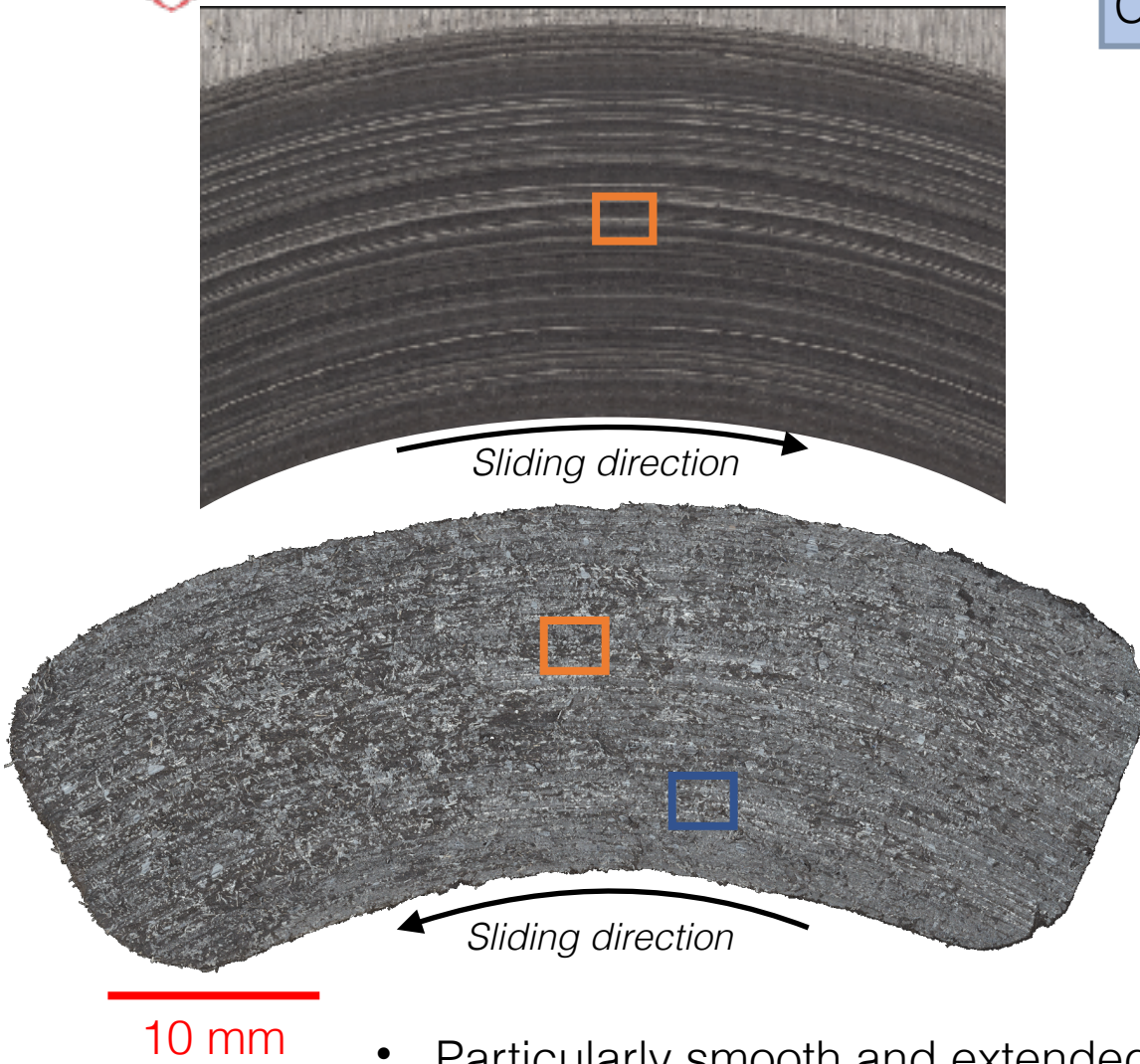


- Similar hot banding phenomena, located in the center of the disc track.
- Fairly similar friction behaviour.

Friction and contact loading cannot explain the difference in particulate emissions behaviour.



Tribological circuit



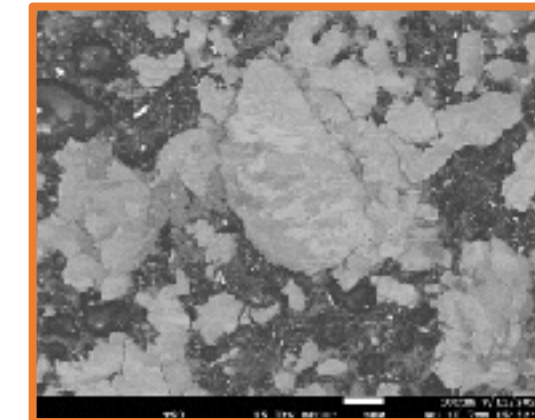
Cast iron

Disc
rubbed
surface

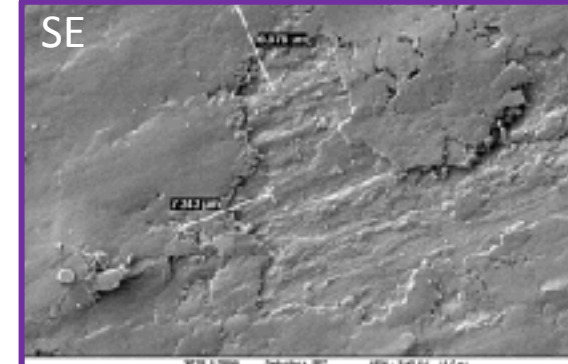
Pad
rubbed
surface



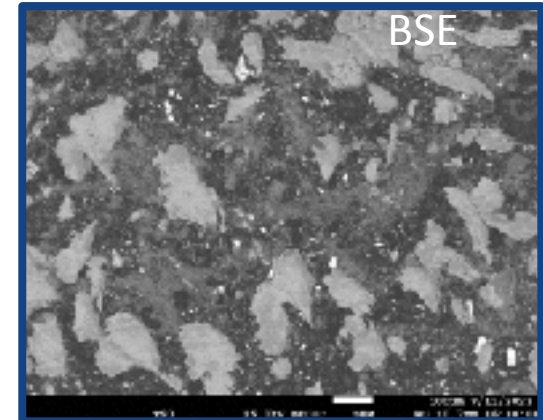
200 µm



200 µm



5 µm



200 µm

High concentration of powdery areas

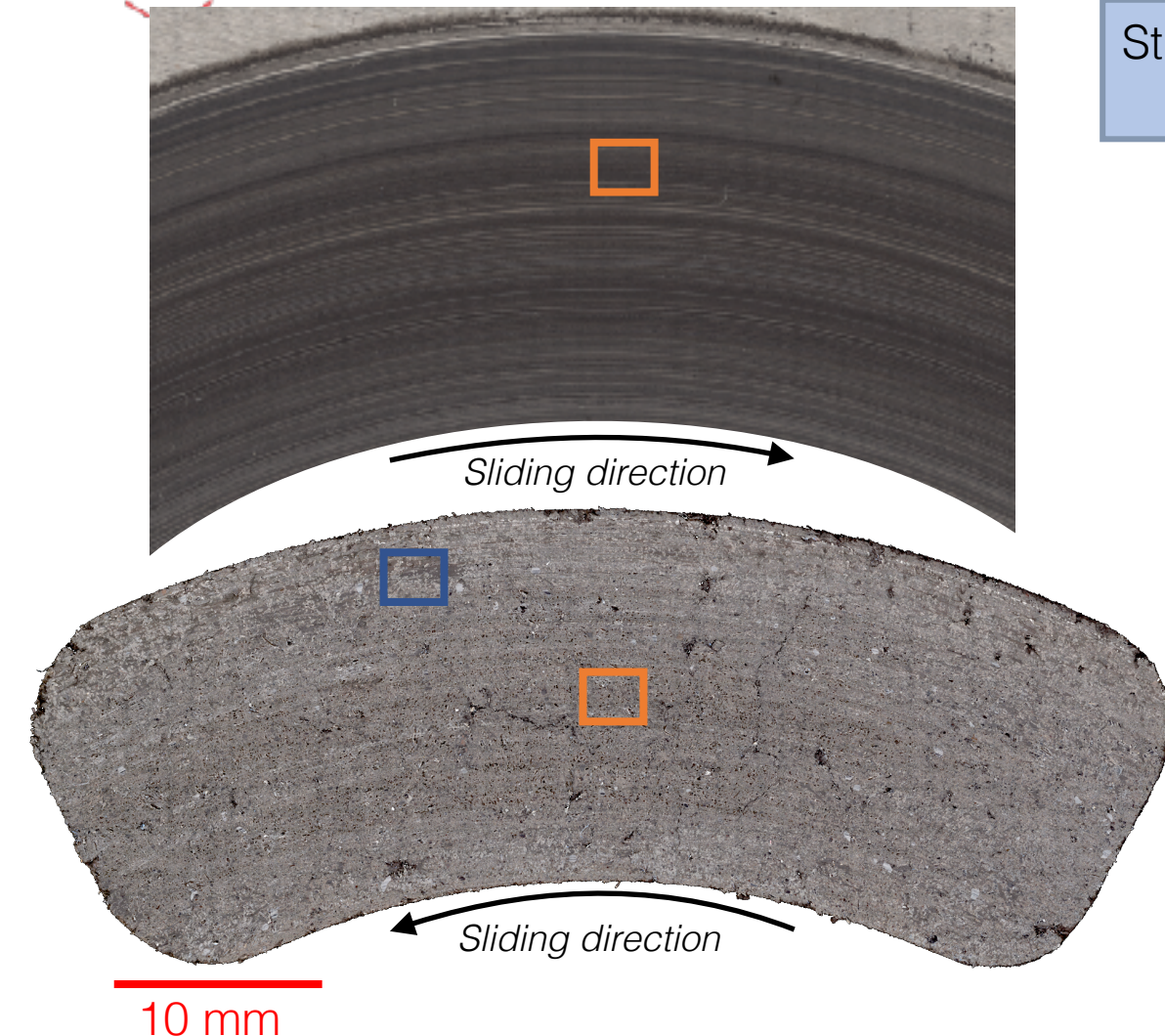
10 mm

- Particularly smooth and extended third-body layer
- Numerous powdery areas (Pad)

→ High third-body flows involved in the tribological circuit



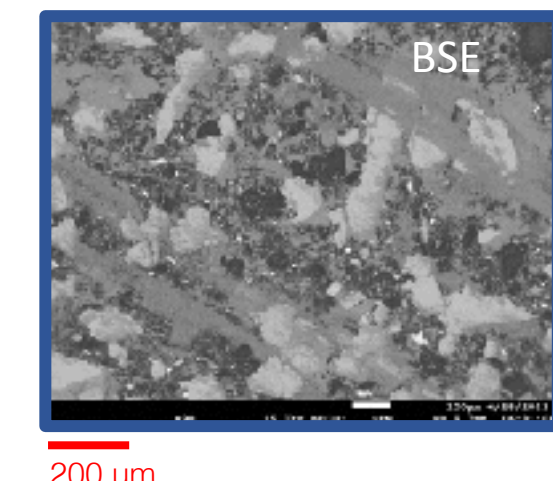
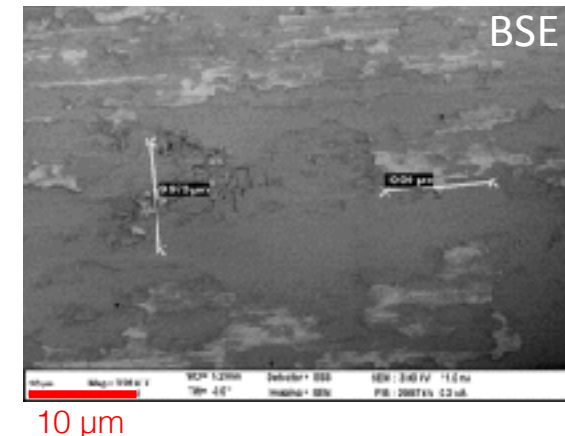
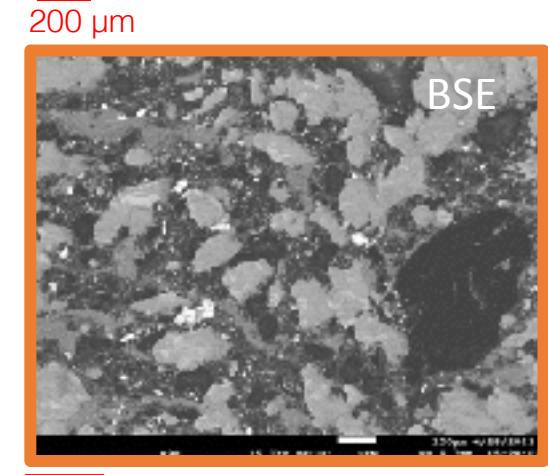
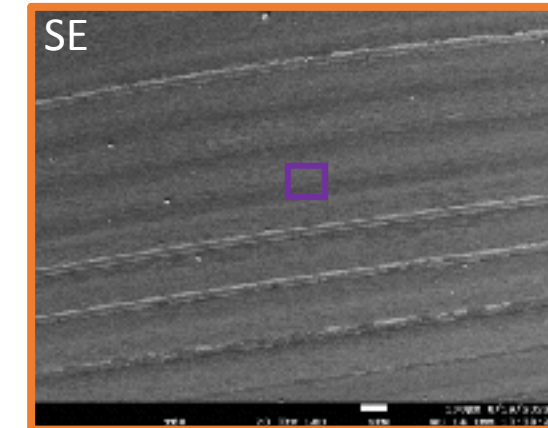
Tribological circuit



Stainless steel

Disc rubbed surface

Pad rubbed surface



Low concentration of powdery areas

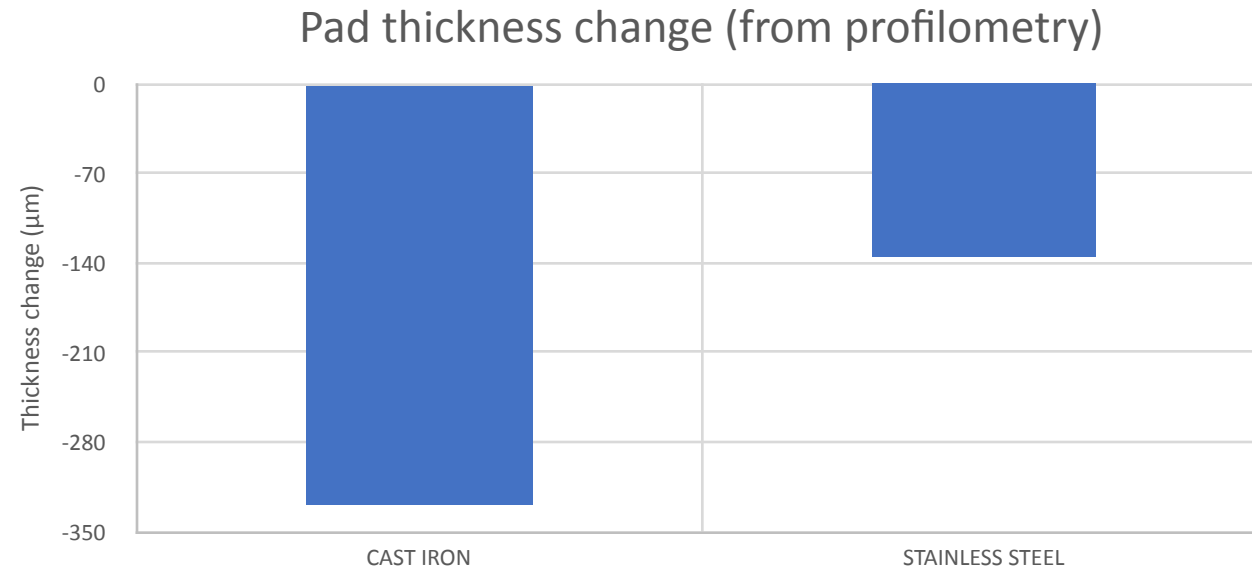
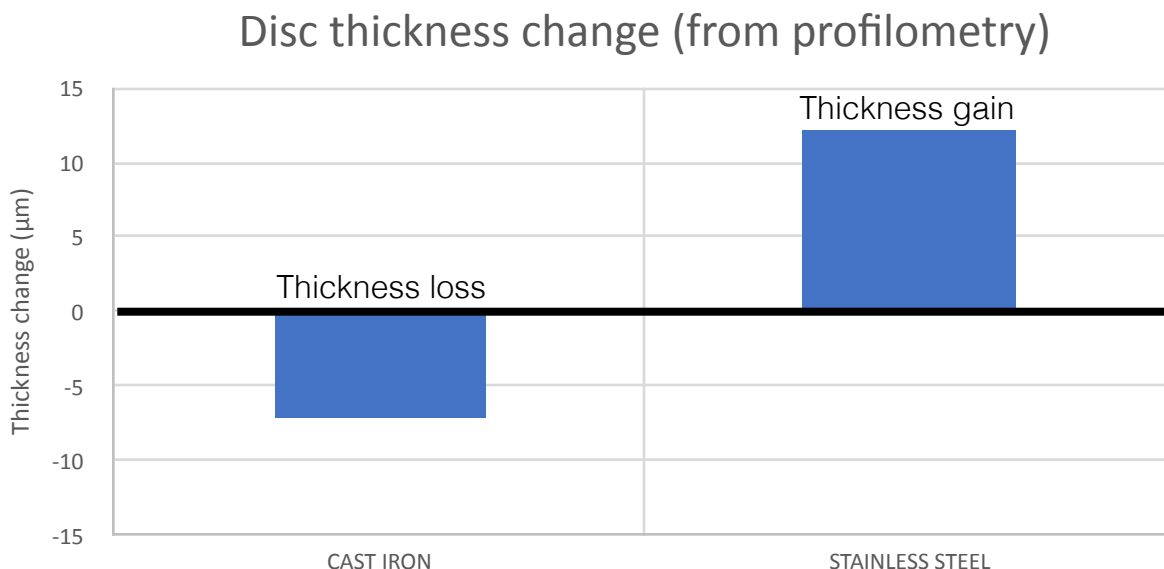
- More structured third-body layer
- Initial disc morphology remains visible: low disc wear rate.

→ low third-body flows involved in the tribological circuit



Tribological circuit

Wear quantification (*disc and pad - include bedding and slowdown series*)



- The change in thickness correlates with the amount of fine particles expelled from the tribological circuit.

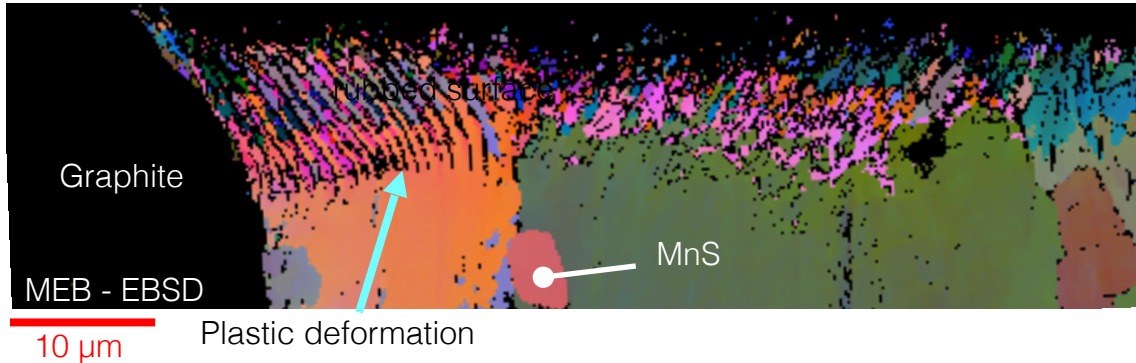
Wear on the pad-disc pair involving a cast-iron disc is much greater than in the case of a steel disc. The high source flow of third body saturates the tribological circuit, which is unable to contain a large quantity of third body, leading to the high level of particle ejection.



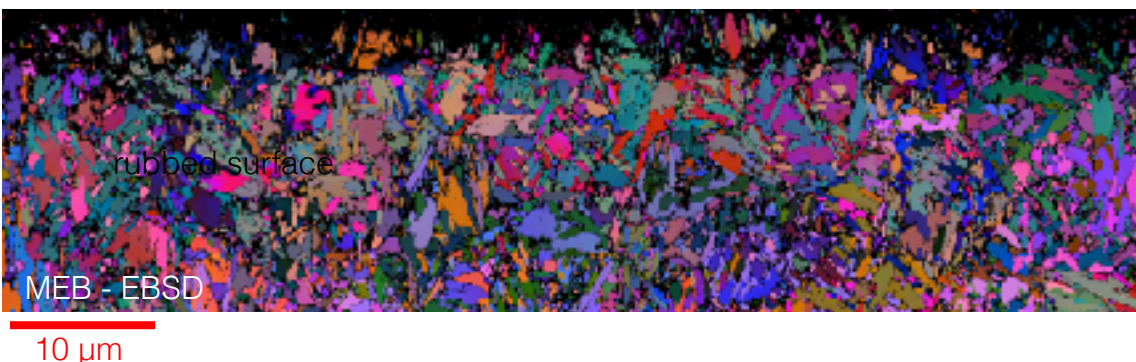
Adaptation des matériaux (disque) Transformations tribologiques de surface

Rubbed sub-surface sections in the hot-band area

Cast iron



Stainless steel



- Significant plastic deformation in the vicinity of graphites and solid lubricant (MnS).
- Reduced grain size very close to the rubbed surface.

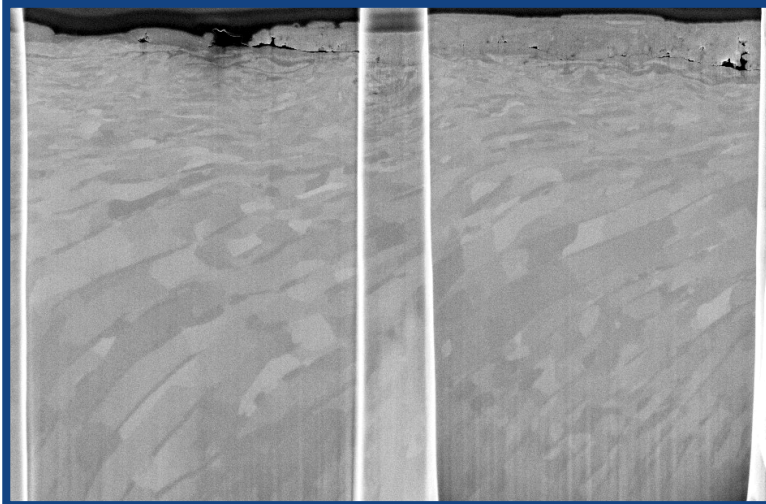


Adaptation des matériaux (disque) Transformations tribologiques de surface

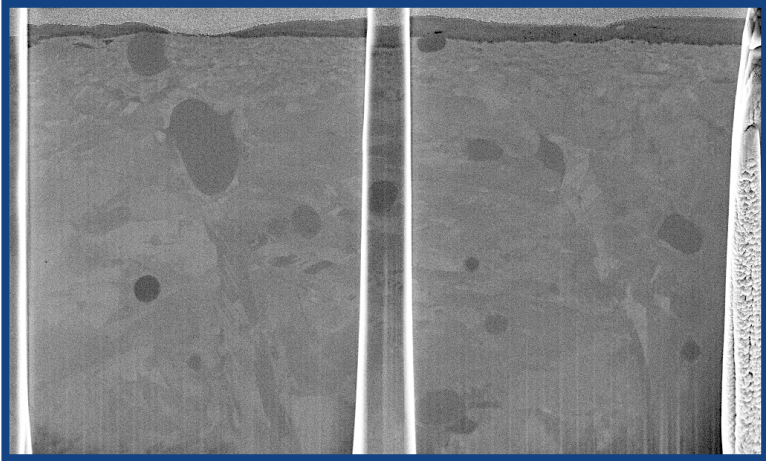
radial direction

sliding direction

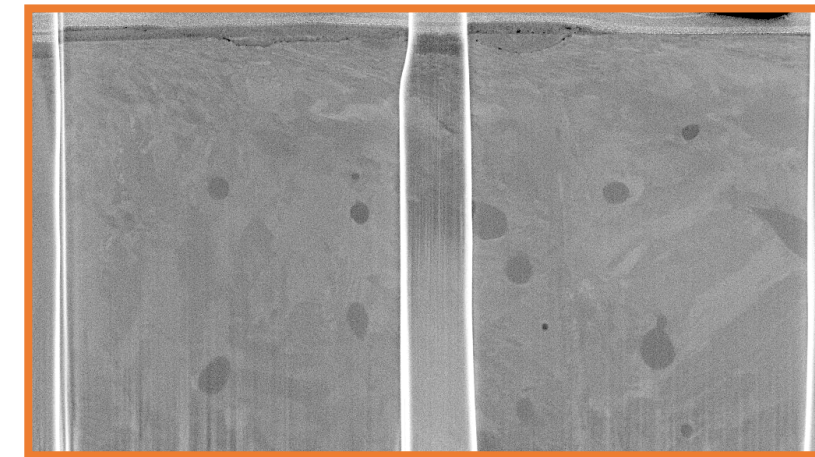
Cast iron



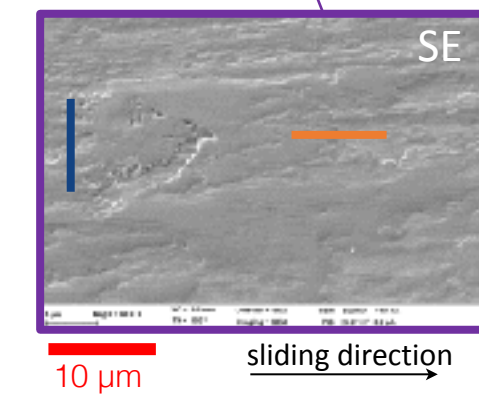
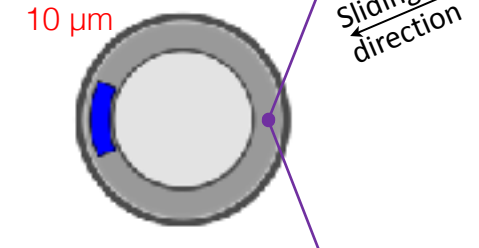
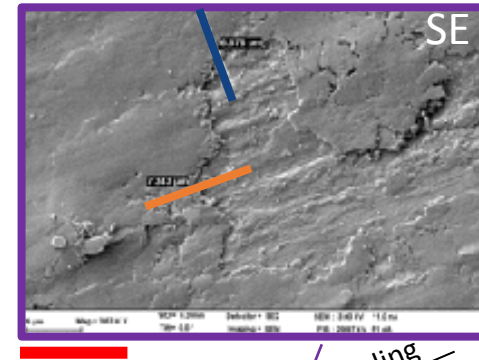
Stainless steel



1 μm



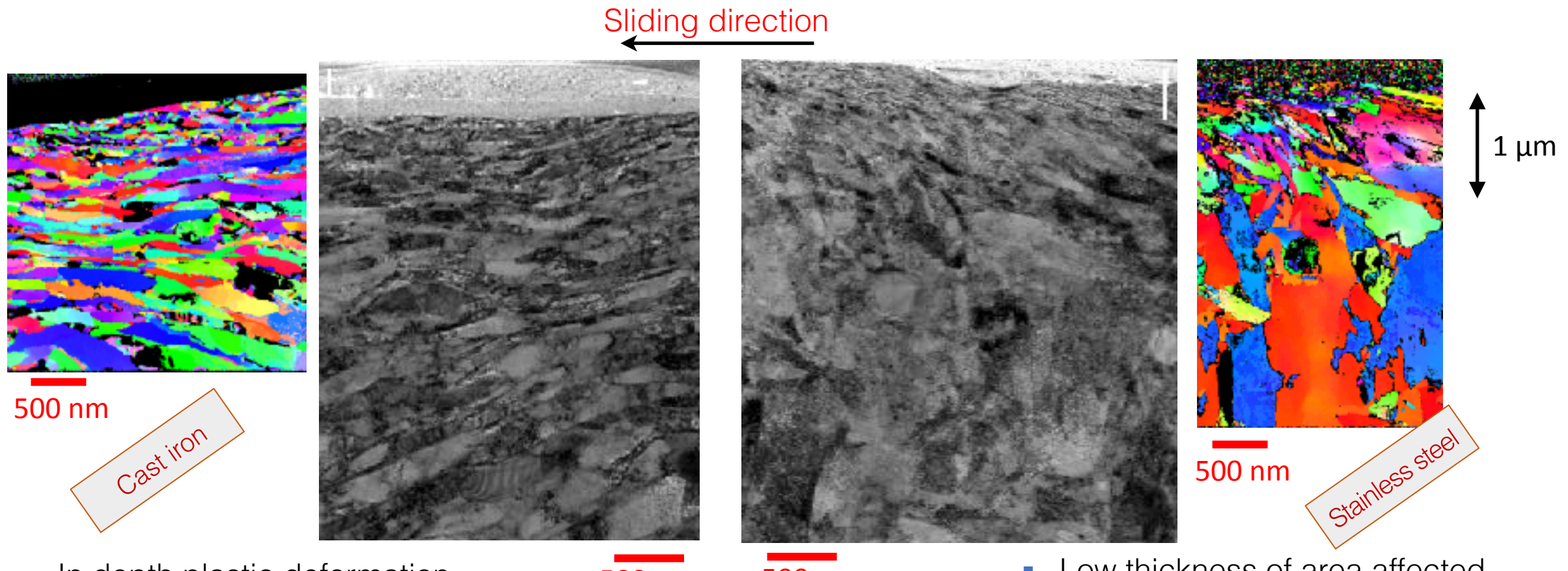
FIB cut location





Adaptation des matériaux (disque)

Transformations tribologiques de surface

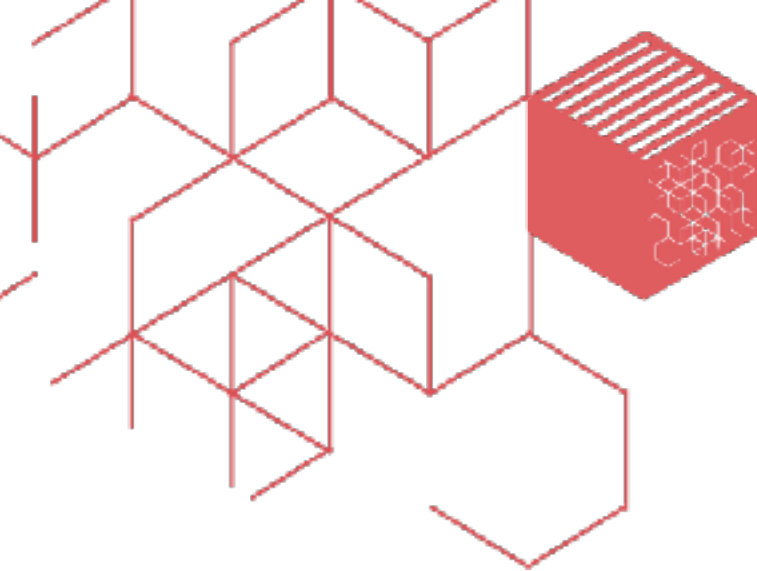


- In depth plastic deformation below the rubbed surface.
 - Nanostructured structure close to the rubbed surface.
 - Plastic flows exist in both sliding and radial directions.
 - No significant phase change observed.
- Low thickness of area affected by plastic deformation



Pour conclure

- Usure et émission en freinage sont interdépendants et dépendent de nombreux facteurs, qui demandent à considérer le système tribologique dans son ensemble :
 - environnement : oxydation, humidité, température...
 - matériaux (disque et garniture) : oxydation, plasticité, tts...
 - usage du frein : régularité, diversité, historique, fréquence d'applications
 - design du frein : localisations thermiques, ouverture et fermeture du contact
- L'usage du système tribologique (frein) détermine le fonctionnement du contact (accommodation de la portance et du glissement, dissipation de l'énergie) par la formation du troisième corps et l'adaptation des matériaux et des surfaces.
- Les émissions dépendent de l'activation des débits de troisième au sein du circuit tribologique. Leur réduction à la source reposent sur le dosage de ces débits et la maîtrise de l'équilibre entre ces débits.



LaM CUBE

Laboratoire de mécanique,
multiphysique, multiéchelle



Journées Tribologie et Traitements de surface
22-23 novembre 2023, CETIM - SENLIS

Merci de votre attention

Acknowledgments:

